Shape optimization under constraints on the probability of a quadratic functional to exceed a given treshold

Marc Dambrine, Giulio Gargantini, Helmut Harbrecht, Jérôme Maynadier

Departement Mathematik und Informatik
Fachbereich Mathematik
Universität Basel
CH-4051 Basel

Preprint No. 2023-13
September 2023

dmi.unibas.ch

Shape optimization under constraints on the probability of a quadratic functional to exceed a given treshold

Marc Dambrine*, Giulio Gargantini*†, Helmut Harbrecht‡, and Jérôme Maynadier†

Abstract. This article is dedicated to shape optimization of elastic materials under random loadings where the particular focus is on the minimization of failure probabilities. Our approach relies on the fact that the area of integration is an ellipsoid in the high-dimensional parameter space when the shape functional of interest is quadratic. We derive the respective expressions for the shape functional and the related shape gradient. As showcase for the numerical implementation, we assume that the random loading is a Gaussian random field. By exploiting the specialties of this setting, we derive an efficient shape optimization algorithm. Numerical results in three spatial dimensions validate the feasibility of our approach.

1. Introduction. In recent decades, shape optimization has been developed as an efficient tool for designing devices which are optimized with respect to a specific purpose. Many practical problems in engineering lead to boundary value problems for an unknown function that must be computed to obtain a desired quantity of interest. In structural mechanics, for example, the equations of linear elasticity form the common model, which are then solved to compute the leading mode of a structure, its compliance, or other quantities. Shape optimization is then applied to optimize the workpiece of interest with respect to this objective functional. We refer the reader to [1, 19, 27, 35, 42] and the references therein for an overview on the topic of shape optimization, which is a subfield of the optimal control of partial differential equations.

The input parameters of the model, like the applied loadings, the material's properties (typically the value of the Young modulus or of the Poisson ratio) or the geometry of the involved shapes itself are usually assumed to be perfectly known. Although this assumption is convenient for the analysis of shape optimization problems, it is unrealistic with regard to applications. In practice, a manufactured component achieves its nominal geometry only up to a tolerance, the material parameters never match the requirements perfectly and the applied forces can only be estimated. Therefore, shape optimization under uncertainty is of great practical interest but started only recently to be investigated, see e.g. [2, 7, 9, 10, 11, 12, 21, 30, 40] for related results.

In this article, we are interested in the solution of a constrained shape optimization problem on a set of mechanical structures subject to a random mechanical loading $\mathbf{g} = \mathbf{g}(\omega)$. Thus, also the state $\mathbf{u}$ becomes a random field, i.e., $\mathbf{u} = \mathbf{u}(\omega)$. The cost functional $\mathcal{Q}(\Omega, \mathbf{g})$ under consideration is supposed to depend quadratically on the state $\mathbf{u}$ (and thus quadratically on $\mathbf{g}$), which covers important functionals such as the compliance or the square norm of the von Mises stresses. The objective is the identification of the structure Ω with the smallest volume for which the probability of failure $\mathbb{P}[\mathcal{Q}(\Omega, \mathbf{g}) > \tau]$ does not exceed a prescribed threshold.

*E2S UPPA, CNRS, LMAP, UMR 5142, Université de Pau et de Pays de l'Adour, Pau, 64000, France.
†Safran Helicopter Engines, Avenue Joseph Szydlowski, Bordes, 64510, France.
‡Department of Mathematics and Computer Science, University of Basel, Basel, Switzerland.

The shape optimization problem under consieration is known to be computationally hard as the probability of failure defines a quantity of interest which is not smooth with respect to the random parameter ω. We are only aware of [2, 9], where this problem has been tackled, however, only by approximating the non-smooth functional by a smooth one. Nonetheless, in the present setting of a quadratic shape functional, we will show that the region, where $\mathcal{Q}(\Omega, \mathbf{g}) > \tau$ holds, is the exterior of an ellipsoid with respect to the stochastic parameter ω. We will exploit this fact in order (i) to compute the shape derivate of the problem under consideration and (ii) to derive an efficient, deterministic shape optimization algorithm.

The rest of this article is structured as follows. In Section 2, we introduce the model problem and compute the shape functional and its shape gradient. Section 3 is then dedicated to our showcase, where we suppose that the loading $\mathbf{g} = \mathbf{g}(\omega)$ is a Gaussian random field. We develop a suitable quadrature formula which can be used to numerically compute the shape functional and the associated shape gradient. Then, in Section 4, we present numerical results in three spatial dimensions in order to demonstrate the feasibility of the present approach. Finally, in Section 5, we state concluding remarks.

2. The shape optimization problem.

2.1. Problem statement. Let us consider a family of Lipschitz continuous admissible domains $\mathcal{S}_{adm}$ in $\mathbb{R}^d$ (for $d = 2$ or 3) sharing the portions Γ_{N} and Γ_{D}, which we suppose to be disjoint. For each $\Omega \in \mathcal{S}_{adm}$, we denote $\Gamma_0 = \partial\Omega \setminus (\Gamma_{\mathrm{N}} \cup \Gamma_{\mathrm{D}})$ the optimizable portion of the boundary. We suppose that the structure to be optimized is made up of a linear elastic material, characterized by the Lamé parameters λ and μ, and is clamped on Γ_{D}.

Let further $(\mathcal{O}, \mathcal{F}, \mathbb{P})$ be a probability space, where $\mathcal{F} \subset 2^{\mathcal{O}}$ is a σ-algebra on $\mathcal{O}$ and $\mathbb{P}$ is a probability measure. A random mechanical load $\mathbf{g} \in \mathrm{L}^2\left(\mathcal{O}, \mathbb{P}; \mathrm{H}^{-1/2}(\Gamma_{\mathrm{N}})\right)$ is applied on the portion Γ_{N} of the boundary. In particular, we suppose that $\mathbf{g}$ can be written in terms of a deterministic term $\overline{\mathbf{g}}_0$ and a finite number N of random terms in accordance with

$$\mathbf{g}(\omega) = \overline{\mathbf{g}}_0 + \overline{\mathbf{g}}_1 X_1(\omega) + \ldots + \overline{\mathbf{g}}_N X_N(\omega) \qquad \text{for almost all } \omega \in \mathcal{O}, \tag{2.1}$$

where $X_1, \ldots, X_N \in \mathrm{L}^2(\mathcal{O}, \mathbb{P}; \mathbb{R})$ are centered and independent, real valued random variables and $\overline{\mathbf{g}}_0, \ldots, \overline{\mathbf{g}}_N \in \mathrm{H}^{-1/2}(\Gamma_{\mathrm{N}})$. Then, for almost any event $\omega \in \mathcal{O}$, the displacement $\mathbf{u}_{\Omega,\mathbf{g}}(\omega) \in \mathrm{H}^1(\Omega)$ is the solution of the following linear elasticity system:

$$\left\{\begin{aligned} -\mathrm{div}\, \boldsymbol{\sigma}(\mathbf{u}_{\Omega,\mathbf{g}}(\omega)) &= \mathbf{0} && \text{in } \Omega, \\ \boldsymbol{\sigma}(\mathbf{u}_{\Omega,\mathbf{g}}(\omega))\mathbf{n} &= \mathbf{0} && \text{on } \Gamma_0, \\ \boldsymbol{\sigma}(\mathbf{u}_{\Omega,\mathbf{g}}(\omega))\mathbf{n} &= \mathbf{g}(\omega) && \text{on } \Gamma_{\mathrm{N}}, \\ \mathbf{u}_{\Omega,\mathbf{g}}(\omega) &= \mathbf{0} && \text{on } \Gamma_{\mathrm{D}}. \end{aligned}\right. \tag{2.2}$$

Here, for any displacement $\mathbf{u} \in \mathrm{H}^1(\Omega)$, $\boldsymbol{\epsilon}(\mathbf{u}) = (\nabla\mathbf{u} + \nabla\mathbf{u}^{\mathrm{T}})/2$ is the infinitesimal strain tensor and $\boldsymbol{\sigma}(\mathbf{u}) = 2\mu\boldsymbol{\epsilon}(\mathbf{u}) + \lambda\, \mathbb{I}\mathrm{div}(\mathbf{u})$ identifies the Cauchy stress tensor.

Throughout this article, we consider the shape optimization problem

$$\left|\begin{array}{l} \text{Find the admissible shape } \Omega \in \mathcal{S}_{adm} \text{ minimizing } \mathrm{Vol}(\Omega) \text{ under the constraint} \\ \qquad \mathbb{P}\left[\langle \mathbf{u}_{\Omega,\mathbf{g}}, Q_\Omega\, \mathbf{u}_{\Omega,\mathbf{g}} \rangle_{\mathrm{H}^1(\Omega)} > \tau\right] \leq \bar{p}, \\ \text{where the state } \mathbf{u}_{\Omega,\mathbf{g}}(\omega) \text{ satisfies the state equation (2.2) for almost all } \omega \in \mathcal{O}. \end{array}\right. \tag{2.3}$$

Note that the value of safety criterion $\mathcal{Q}(\Omega, \mathbf{g})$ is supposed to be a quadratic functional of the displacement $\mathbf{u}_{\Omega,\mathbf{g}}$. As we intend to adopt the moving boundary approach developed by Hadamard in order to solve this shape optimization problem (see e.g. [1, 42, 27]), we require that, for any $\mathbf{g} \in \mathrm{H}^{-1/2}(\Gamma_{\mathrm{N}})$, the mapping $\Omega \mapsto \mathcal{Q}(\Omega, \mathbf{g})$ is differentiable with respect to the shape (we refer to [27, Chapter 5] for the complete definition of differentiability with respect to a moving domain).

2.2. Properties of the safety criterion. We shall highlight the dependency of the constraint $\mathbb{P}\left[\langle \mathbf{u}_{\Omega,\mathbf{g}}, Q_\Omega\, \mathbf{u}_{\Omega,\mathbf{g}} \rangle_{\mathrm{H}^1(\Omega)} > \tau\right]$ from the random variables $X_1, \ldots, X_N$ appearing in the definition (2.1) of the mechanical load. For all $i \in \{1, \ldots, N\}$, we define the displacement $\mathbf{u}_{\Omega,i} \in \mathrm{H}^1(\Omega)$ as the solution of the following deterministic elasticity problem:

$$\begin{cases} -\mathrm{div}\, \boldsymbol{\sigma}(\mathbf{u}_{\Omega,i}) &= \mathbf{0} & \text{in } \Omega, \\ \boldsymbol{\sigma}(\mathbf{u}_{\Omega,i})\mathbf{n} &= \mathbf{0} & \text{on } \Gamma_0, \\ \boldsymbol{\sigma}(\mathbf{u}_{\Omega,i})\mathbf{n} &= \overline{\mathbf{g}}_i & \text{on } \Gamma_{\mathrm{N}}, \\ \mathbf{u}_{\Omega,i} &= \mathbf{0} & \text{on } \Gamma_{\mathrm{D}}. \end{cases}$$

Thanks to the linearity of the state equation (2.2), the displacement $\mathbf{u}_{\Omega,\mathbf{g}} \in \mathrm{L}^2\left(\mathcal{O}, \mathbb{P}; \mathrm{H}^1(\Omega)\right)$ can be written as a sum of N terms, depending from the same random variables as in (2.1):

$$\mathbf{u}_{\Omega,\mathbf{g}}(\omega) = \mathbf{u}_{\Omega,0} + \mathbf{u}_{\Omega,1} X_1(\omega) + \ldots + \mathbf{u}_{\Omega,N} X_N(\omega) \qquad \text{for almost all } \omega \in \mathcal{O}. \tag{2.4}$$

Since the safety functional is quadratic with respect to the displacement, we can express it as a quadratic function $\Psi_\Omega : \mathbb{R}^N \to \mathbb{R}$ of the random vector $\mathbf{X} = (X_1, \ldots, X_N) \in \mathrm{L}^2\left(\mathcal{O}, \mathbb{P}; \mathbb{R}^N\right)$ as

$$\mathcal{Q}(\Omega, \mathbf{g}(\omega)) = \Psi_\Omega(\mathbf{X}(\omega)) = \mathbf{X}(\omega)^{\mathrm{T}} \mathbf{M}_\Omega\, \mathbf{X}(\omega) + 2{\mathbf{b}_\Omega}^{\mathrm{T}} \mathbf{X}(\omega) + c_\Omega, \tag{2.5}$$

for almost all $\omega \in \mathcal{O}$. The symmetric matrix $\mathbf{M}_\Omega \in \mathrm{Sym}_N \subset \mathbb{R}^{N\times N}$, the vector $\mathbf{b}_\Omega \in \mathbb{R}^N$, and the scalar c_Ω are functions of the displacements $\mathbf{u}_{\Omega,1}, \ldots, \mathbf{u}_{\Omega,N}$, and are defined as

- $[\mathbf{M}_\Omega]_{i,j} = \langle \mathbf{u}_{\Omega,i}, Q_\Omega\, \mathbf{u}_{\Omega,j} \rangle_{\mathrm{H}^1(\Omega)}$ for all $i, j \in \{1, \ldots, N\}$;
- $[\mathbf{b}_\Omega]_k = \langle \mathbf{u}_{\Omega,0}, Q_\Omega\, \mathbf{u}_{\Omega,k} \rangle_{\mathrm{H}^1(\Omega)}$ for all $k \in \{1, \ldots, N\}$;
- $c_\Omega = \langle \mathbf{u}_{\Omega,0}, Q_\Omega\, \mathbf{u}_{\Omega,0} \rangle_{\mathrm{H}^1(\Omega)}$.

Since Q_Ω is a self-adjoint positive definite operator, the matrix $\mathbf{M}_\Omega$ is symmetric having N eigenvalues $\lambda_{\Omega,1}, \ldots, \lambda_{\Omega,N}$ that are real and strictly positive.

Let us consider the (deterministic) subset of $\mathbb{R}^N$ $\mathcal{E}(\Psi_\Omega, \tau)$ containing all the realizations of the random vector $\mathbf{X}$ for which the constraint is satisfied:

$$\mathcal{E}(\Psi_\Omega, \tau) = \left\{ \mathbf{x} \in \mathbb{R}^N \,:\, \Psi_\Omega(\mathbf{x}) \leq \tau \right\}. \tag{2.6}$$

We denote $\widetilde{\tau}_\Omega$ the following quantity:

$$\widetilde{\tau}_\Omega = \tau - \left(c_\Omega - {\mathbf{b}_\Omega}^{\mathrm{T}} {\mathbf{M}_\Omega}^{-1} \mathbf{b}_\Omega \right). \tag{2.7}$$

Given the properties of the quadratic function Ψ_Ω and assuming that $\widetilde{\tau}_\Omega > 0$, we recognize that $\mathcal{E}(\Psi_\Omega, \tau)$ is an ellipsoid in $\mathbb{R}^N$, centered in $-{\mathbf{M}_\Omega}^{-1} \mathbf{b}_\Omega$, and whose semi-axes are oriented as the eigenvectors of $\mathbf{M}_\Omega$ and have length $r_1^{\Omega,\tau}, \ldots, r_N^{\Omega,\tau}$:

$$r_i^{\Omega,\tau} = \sqrt{\widetilde{\tau}_\Omega / \lambda_{\Omega,i}} \qquad \text{for all } i \in \{1, \ldots, N\}. \tag{2.8}$$

However, if $\widetilde{\tau}_\Omega < 0$, we have that $\mathcal{E}(\Psi_\Omega, \tau) = \emptyset$, and the constraint cannot be satisfied if $\bar{p} < 1$.

For the sake of clarity, we introduce the shape functional $\Phi : \mathcal{S}_{adm} \to \mathbb{R}$ defined as the probability of the constraint to be satisfied:

$$\Phi(\Omega) = \mathbb{P}[\mathcal{Q}(\Omega, \mathbf{g}) \leq \tau] = 1 - \mathbb{P}[\mathcal{Q}(\Omega, \mathbf{g}) > \tau].$$

The inequality constraint in problem (2.3) can be written alternatively as $\Phi(\Omega) \geq 1 - \bar{p}$. Especially, $\Phi(\Omega)$ can be expressed by means of the probability for the random vector $\mathbf{X}$ to belong to the ellipsoid $\mathcal{E}(\Psi_\Omega, \tau)$

$$\Phi(\Omega) = \mathbb{P}[\Psi_\Omega(\mathbf{X}) \leq \tau] = \mathbb{P}[\mathbf{X} \in \mathcal{E}(\Psi_\Omega, \tau)].$$

Therefore, $\Phi(\Omega)$ can be interpreted as the volume of the ellipsoid $\mathcal{E}(\Psi_\Omega, \tau)$ with respect to the probability measure $\mathbb{P}_\mathbf{X}$ induced by the random variable $\mathbf{X}$:

$$\Phi(\Omega) = \mathbb{P}[\mathbf{X} \in \mathcal{E}(\Psi_\Omega, \tau)] = \mathbb{P}_\mathbf{X}(\mathcal{E}(\Psi_\Omega, \tau)) = \int_{\mathcal{E}(\Psi_\Omega, \tau)} 1 \, \mathrm{d}\mathbb{P}_\mathbf{X}(\mathbf{x}). \tag{2.9}$$

2.3. Sensitivity of the exceeding probability. In order to solve problem (2.3) using a gradient-based optimization algorithm, we have to compute an expression for $\Phi(\Omega)$ and for its shape derivative $\frac{\mathrm{d}}{\mathrm{d}\Omega}[\Phi(\Omega)](\cdot)$. To this end, let us suppose that the random vector $\mathbf{X}$ admits a probability density function $f : \mathbb{R}^N \to \mathbb{R}^+$, such that $f \in \mathrm{W}^{1,1}(\mathbb{R}^N)$. Then, in view of (2.9), the quantity $\Phi(\Omega)$ can be written as:

$$\Phi(\Omega) = \int_{\mathcal{E}(\Psi_\Omega, \tau)} f(\mathbf{x}) \, \mathrm{d}\mathbf{x} \tag{2.10}$$

Moreover, we suppose that all entries of $\mathbf{M}_\Omega$ and $\mathbf{b}_\Omega$, as well as c_Ω are differentiable with respect to the shape, and we denote their shape derivatives by $\frac{\mathrm{d}}{\mathrm{d}\Omega}[\mathbf{M}_\Omega](\boldsymbol{\theta})$, $\frac{\mathrm{d}}{\mathrm{d}\Omega}[\mathbf{b}_\Omega](\boldsymbol{\theta})$, and $\frac{\mathrm{d}}{\mathrm{d}\Omega}[c_\Omega](\boldsymbol{\theta})$, respectively.

We recognize in (2.10) the expression of the integral of a constant function over a variable domain $\mathcal{E}(\Psi_\Omega, \tau)$. Let $\boldsymbol{\xi} \in \mathrm{W}^{1,\infty}(\mathbb{R}^N; \mathbb{R}^N)$ be a Lipschitz continuous deformation field in $\mathbb{R}^N$. Then, we can compute the derivative of the mapping $\boldsymbol{\xi} \mapsto \mathbb{P}[\mathbf{X} \in \mathcal{E}(\Psi_\Omega, \tau) \circ (\mathbb{I} + \boldsymbol{\xi})]$ thanks to the usual shape differentiation techniques (see [27, Eq. (5.24)]). Moreover, since $\mathcal{E}(\Psi_\Omega, \tau)$ is an ellipsoid and supposing that $\boldsymbol{\xi}$ is also $\mathcal{C}^1$, we can apply Hadamard's regularity theorem (see [27, Proposition 5.9.1]) and write

$$\begin{aligned} \frac{\mathrm{d}}{\mathrm{d}\tilde{\boldsymbol{\xi}}} \mathbb{P}\left[\mathbf{X} \in \mathcal{E}(\Psi_\Omega, \tau) \circ (\mathbb{I} + \tilde{\boldsymbol{\xi}})\right]\Big|_{\tilde{\boldsymbol{\xi}}=0} (\boldsymbol{\xi}) &= \int_{\mathcal{E}(\Psi_\Omega, \tau)} \operatorname{div} \boldsymbol{\xi}(\mathbf{x}) \, f(\mathbf{x}) \, \mathrm{d}\mathbf{x} \\ &= \int_{\partial\mathcal{E}(\Psi_\Omega, \tau)} f(\mathbf{s}) \left(\boldsymbol{\xi}(\mathbf{s}) \cdot \mathbf{n}(\mathbf{s})\right) \mathrm{d}\mathbf{s}. \end{aligned} \tag{2.11}$$

Here, for all $\mathbf{s} \in \partial\mathcal{E}(\Psi_\Omega, \tau)$, $\mathbf{n}(\mathbf{s}) \in \mathbb{R}^N$ is the unitary vector orthogonal to $\partial\mathcal{E}(\Psi_\Omega, \tau)$ in $\mathbf{s}$.

Lemma 2.1. *Let us consider an admissible domain $\Omega \in \mathcal{S}_{adm}$ and a regular enough displacement field $\boldsymbol{\theta} \in \mathcal{C}^1 \cap \mathrm{W}^{1,\infty}\left(\mathbb{R}^d;\mathbb{R}^d\right)$ for the domain Ω such that $\|\boldsymbol{\theta}\|_\infty < 1$. We denote $\boldsymbol{\Xi}_{\Omega,\boldsymbol{\theta}} \in \mathbb{R}^{N\times N}$ and $\mathbf{r}_{\Omega,\boldsymbol{\theta}} \in \mathbb{R}^N$ the matrix and the vector respectively defined as*

$$\boldsymbol{\Xi}_{\Omega,\boldsymbol{\theta}} = \frac{\frac{\mathrm{d}}{\mathrm{d}\Omega}\left[\widetilde{\tau}_\Omega\right](\boldsymbol{\theta})}{2\widetilde{\tau}_\Omega}\mathbb{I} - \frac{1}{2}\mathbf{M}_\Omega{}^{-1}\frac{\mathrm{d}}{\mathrm{d}\Omega}\left[\mathbf{M}_\Omega\right](\boldsymbol{\theta})\,; \tag{2.12}$$

$$\mathbf{r}_{\Omega,\boldsymbol{\theta}} = -\mathbf{M}_\Omega{}^{-1}\frac{\mathrm{d}}{\mathrm{d}\Omega}\left[\mathbf{b}_\Omega\right](\boldsymbol{\theta}) + \left(\frac{\frac{\mathrm{d}}{\mathrm{d}\Omega}\left[\widetilde{\tau}_\Omega\right](\boldsymbol{\theta})}{2\widetilde{\tau}_\Omega}\mathbb{I} + \frac{1}{2}\mathbf{M}_\Omega{}^{-1}\frac{\mathrm{d}}{\mathrm{d}\Omega}\left[\mathbf{M}_\Omega\right](\boldsymbol{\theta})\right)\mathbf{M}_\Omega{}^{-1}\mathbf{b}_\Omega, \tag{2.13}$$

where $\frac{\mathrm{d}}{\mathrm{d}\Omega}\left[\widetilde{\tau}_\Omega\right](\boldsymbol{\theta})$ has the expression

$$\frac{\mathrm{d}}{\mathrm{d}\Omega}\left[\widetilde{\tau}_\Omega\right](\boldsymbol{\theta}) = -\frac{\mathrm{d}}{\mathrm{d}\Omega}\left[c_\Omega\right](\boldsymbol{\theta}) - \mathbf{M}_\Omega{}^{-1}\frac{\mathrm{d}}{\mathrm{d}\Omega}\left[\mathbf{M}_\Omega\right](\boldsymbol{\theta})\,\mathbf{M}_\Omega{}^{-1}\mathbf{b}_\Omega + \mathbf{M}_\Omega{}^{-1}\frac{\mathrm{d}}{\mathrm{d}\Omega}\left[\mathbf{b}_\Omega\right](\boldsymbol{\theta})\,. \tag{2.14}$$

Then, $\boldsymbol{\xi}^{\boldsymbol{\theta}} : \mathbf{x} \mapsto \boldsymbol{\Xi}_{\Omega,\boldsymbol{\theta}}\,\mathbf{x} + \mathbf{r}_{\Omega,\boldsymbol{\theta}}$ is a $\mathcal{C}^1$ Lipschitz-continuous displacement field on $\mathbb{R}^N$ such that the shape derivative of $\Phi(\cdot)$ in Ω can be written in its volumic and surface forms as

$$\frac{\mathrm{d}}{\mathrm{d}\Omega}\left[\Phi(\Omega)\right](\boldsymbol{\theta}) = \int_{\mathcal{E}(\Psi_\Omega,\tau)} \operatorname{div}\left(f(\mathbf{x})\boldsymbol{\xi}^{\boldsymbol{\theta}}(\mathbf{x})\right)\mathrm{d}\mathbf{x} = \int_{\partial\mathcal{E}(\Psi_\Omega,\tau)} f(\mathbf{s})\left(\boldsymbol{\xi}^{\boldsymbol{\theta}}(\mathbf{s})\cdot\mathbf{n}(\mathbf{s})\right)\mathrm{d}\mathbf{s}. \tag{2.15}$$

Proof. Let $\delta > 0$ be such that, for any $t \in [0,\delta]$, $\widetilde{\tau}_{\Omega\circ(\mathbb{I}+t\boldsymbol{\theta})} > 0$. We consider the following dynamical system:

$$\left\{\begin{array}{lcll} \dot{\mathbf{x}}(t;\bar{\mathbf{x}}) & = & \boldsymbol{\Xi}_{\Omega\circ(\mathbb{I}+t\boldsymbol{\theta}),\boldsymbol{\theta}}\mathbf{x}(t;\bar{\mathbf{x}}) + \mathbf{r}_{\Omega\circ(\mathbb{I}+t\boldsymbol{\theta}),\boldsymbol{\theta}} & \text{for } t \in [0,\delta], \bar{\mathbf{x}} \in \mathbb{R}^N, \\ \mathbf{x}(0;\bar{\mathbf{x}}) & = & \bar{\mathbf{x}} & \text{for } \bar{\mathbf{x}} \in \mathbb{R}^N. \end{array}\right. \tag{2.16}$$

We set

$$\mathbf{y}(t,\theta,\bar{\mathbf{x}}) := \mathbf{x}(t;\bar{\mathbf{x}}) + \mathbf{M}_{\Omega\circ(\mathbb{I}+t\boldsymbol{\theta})}{}^{-1}\mathbf{b}_{\Omega\circ(\mathbb{I}+t\boldsymbol{\theta})}$$

and remark that the quantity defined as

$$\mathfrak{F}_{\Omega\circ(\mathbb{I}+t\boldsymbol{\theta})}\big(\mathbf{y}(t,\theta,\bar{\mathbf{x}})\big) = \frac{\mathbf{y}(t,\theta,\bar{\mathbf{x}})^{\mathrm{T}}\mathbf{M}_{\Omega\circ(\mathbb{I}+t\boldsymbol{\theta})}\mathbf{y}(t,\theta,\bar{\mathbf{x}})}{\widetilde{\tau}_{\Omega\circ(\mathbb{I}+t\boldsymbol{\theta})}}$$

is constant along the trajectories. Indeed, using the expressions (2.12), (2.13), and (2.16), there holds

$$\begin{aligned} \frac{\mathrm{d}}{\mathrm{d}t}\mathfrak{F}_{\Omega\circ(\mathbb{I}+t\boldsymbol{\theta})}\big(\mathbf{y}(t,\theta,\bar{\mathbf{x}})\big) = \widetilde{\tau}^{-2}_{\Omega\circ(\mathbb{I}+t\boldsymbol{\theta})}\Bigg[&- \frac{\mathrm{d}}{\mathrm{d}\Omega}\left[\widetilde{\tau}_{\Omega\circ(\mathbb{I}+t\boldsymbol{\theta})}\right](\boldsymbol{\theta})\;\mathbf{y}(t,\theta,\bar{\mathbf{x}})^{\mathrm{T}}\mathbf{M}_{\Omega\circ(\mathbb{I}+t\boldsymbol{\theta})}\mathbf{y}(t,\theta,\bar{\mathbf{x}}) \\ &+ \widetilde{\tau}_{\Omega\circ(\mathbb{I}+t\boldsymbol{\theta})}\Bigg(\mathbf{y}(t,\theta,\bar{\mathbf{x}})^{\mathrm{T}}\frac{\mathrm{d}}{\mathrm{d}t}\mathbf{M}_{\Omega\circ(\mathbb{I}+t\boldsymbol{\theta})}\mathbf{y}(t,\theta,\bar{\mathbf{x}}) + 2\mathbf{y}(t,\theta,\bar{\mathbf{x}})^{\mathrm{T}} \\ &\times\left(\mathbf{M}_{\Omega\circ(\mathbb{I}+t\boldsymbol{\theta})}\dot{\mathbf{x}}(t;\bar{\mathbf{x}}) - \frac{\mathrm{d}}{\mathrm{d}t}\mathbf{M}_{\Omega\circ(\mathbb{I}+t\boldsymbol{\theta})}\mathbf{M}_{\Omega\circ(\mathbb{I}+t\boldsymbol{\theta})}{}^{-1}\mathbf{b}_{\Omega\circ(\mathbb{I}+t\boldsymbol{\theta})} + \frac{\mathrm{d}}{\mathrm{d}t}\mathbf{b}_{\Omega\circ(\mathbb{I}+t\boldsymbol{\theta})}\right)\Bigg)\Bigg] = 0. \end{aligned}$$

Moreover, for any $t \in [1,\delta]$, the inequality $\mathfrak{F}_{\Omega\circ(\mathbb{I}+t\boldsymbol{\theta})}(\mathbf{x}) \leq 1$ defines the same ellipsoid $\mathcal{E}\left(\Psi_{\Omega\circ(\mathbb{I}+t\boldsymbol{\theta})},\tau\right)$ as the inequality $\Psi_{\Omega\circ(\mathbb{I}+t\boldsymbol{\theta})}(\mathbf{x}) \leq \tau$. Therefore, the deformation $\mathbf{x} \mapsto (\mathbb{I} + \mathcal{F}_t)\,\mathbf{x}$

gives the identity $\mathcal{E}\left(\Psi_{\Omega\circ(\mathbb{I}+t\boldsymbol{\theta})},\tau\right) = \mathcal{E}\left(\Psi_\Omega,\tau\right)\circ\left(\mathbb{I}+\mathcal{F}_t\right)$, where $\mathcal{F}_t:\mathbb{R}^N\to\mathbb{R}^N$ is defined as $\mathcal{F}_t\,\mathbf{x} = \int_0^t \dot{\mathbf{x}}(s;\mathbf{x})\mathrm{d}s$ for $t\in[0,\delta]$.

We recall that, for any differentiable shape functional F and Lipschitz-continuous domain $D\in\mathbb{R}^N$, we have

$$\frac{\mathrm{d}}{\mathrm{d}t}F\Big(D\circ\left(\mathbb{I}+\boldsymbol{\xi}(t)\right)\Big)\Big|_{t=0} = \frac{\mathrm{d}}{\mathrm{d}D}F(D)\left(\boldsymbol{\xi}'(0)\right), \tag{2.17}$$

provided that $\boldsymbol{\xi}:[0,\delta]\to\mathrm{W}^{1,\infty}\left(\mathbb{R}^N;\mathbb{R}^N\right)$ is a differentiable mapping that vanishes in $t=0$. Therefore, since $\frac{\mathrm{d}}{\mathrm{d}t}\mathcal{F}_t\big|_{t=0} = \dot{\mathbf{x}}(0,\mathbf{x}) = \boldsymbol{\Xi}_{\Omega,\boldsymbol{\theta}}\mathbf{x}+\mathbf{r}_{\Omega,\boldsymbol{\theta}} = \boldsymbol{\xi}^{\boldsymbol{\theta}}(\mathbf{x})$, we conclude that

$$\begin{aligned}
\frac{\mathrm{d}}{\mathrm{d}\Omega}\left[\Phi\left(\Omega\right)\right](\boldsymbol{\theta}) &= \frac{\mathrm{d}}{\mathrm{d}t}\Phi\left(\Omega\circ\left(\mathbb{I}+t\boldsymbol{\theta}\right)\right)\Big|_{t=0} = \frac{\mathrm{d}}{\mathrm{d}t}\int_{\mathcal{E}\left(\mathbf{M}_{\Omega\circ(\mathbb{I}+t\boldsymbol{\theta})},\tau\right)} f(\mathbf{x})\,\mathrm{d}\mathbf{x}\Big|_{t=0}\\
&= \frac{\mathrm{d}}{\mathrm{d}t}\int_{\mathcal{E}(\Psi_\Omega,\tau)\circ(\mathbb{I}+\mathcal{F}_t)} f(\mathbf{x})\,\mathrm{d}\mathbf{x}\Big|_{t=0} = \int_{\mathcal{E}(\Psi_\Omega,\tau)}\mathrm{div}\,\Big(f(\mathbf{x})\,\boldsymbol{\xi}^{\boldsymbol{\theta}}(\mathbf{x})\Big)\,\mathrm{d}\mathbf{x}\\
&= \int_{\partial\mathcal{E}(\Psi_\Omega,\tau)} f(\mathbf{s})\left(\mathbf{n}(\mathbf{s})\cdot\boldsymbol{\xi}^{\boldsymbol{\theta}}(\mathbf{s})\right)\mathrm{d}\mathbf{s}. \qquad\blacksquare
\end{aligned}$$

A first remark on the result of Lemma 2.1 is that, since $\boldsymbol{\xi}^{\boldsymbol{\theta}}(\mathbf{x})$ is a linear function of $\boldsymbol{\theta}$, the expression we found is a Fréchet derivative of the functional $\Phi(\cdot)$. A second observation concerns the expression of the derivative as a surface integral on a variable ellipsoid. For numerical reasons, it might be more interesting to reformulate the integral as one on a fixed domain. Thus, we can use the volumic expression of the shape derivative to write (2.15) as an integral on the unitary N-sphere, as is done in the following proposition.

Proposition 2.2. *Under the hypotheses of Lemma 2.1, the shape derivative of the functional $\Phi(\cdot)$ in Ω can be written as an integral on the unit N-sphere $\mathbb{S}_{N-1}$ in accordance with*

$$\begin{aligned}
\frac{\mathrm{d}}{\mathrm{d}\Omega}\left[\Phi\left(\Omega\right)\right](\boldsymbol{\theta}) = \sqrt{\frac{\widetilde{\tau}_\Omega^N}{\det\mathbf{M}_\Omega}}\int_{\mathbb{S}_{N-1}} & f\left(\sqrt{\widetilde{\tau}_\Omega}\mathbf{M}_\Omega{}^{-1/2}\mathbf{s}-\mathbf{M}_\Omega{}^{-1}\mathbf{b}_\Omega\right)\\
&\times\left(\left(\boldsymbol{\Xi}_{\Omega,\boldsymbol{\theta}}\mathbf{M}_\Omega{}^{-1/2}\mathbf{s}+\frac{1}{\sqrt{\widetilde{\tau}_\Omega}}\left(\mathbf{r}_{\Omega,\boldsymbol{\theta}}-\boldsymbol{\Xi}_{\Omega,\boldsymbol{\theta}}\mathbf{M}_\Omega{}^{-1}\mathbf{b}_\Omega\right)\right)\cdot\left(\mathbf{M}_\Omega{}^{1/2}\mathbf{s}\right)\right)\mathrm{d}\mathbf{s}.
\end{aligned} \tag{2.18}$$

Proof. In order to prove (2.18), we consider the expression of the shape derivative given by Lemma 2.1 and apply the change of variables such that $\mathbf{y} = \frac{1}{\sqrt{\widetilde{\tau}_\Omega}}\mathbf{M}_\Omega{}^{1/2}\left(\mathbf{x}+\mathbf{M}_\Omega{}^{-1}\mathbf{b}_\Omega\right)$, mapping $\mathcal{E}\left(\Psi_\Omega,\tau\right)$ to $\mathbb{B}_N$. We recall that, for any function $\mathbf{f}:\mathbb{R}^N\to\mathbb{R}^N$ that is $\mathcal{C}^1(\mathcal{A})$ in a given open subset $\mathcal{A}$ of $\mathbb{R}^N$, the expression of the divergence with respect to the variable $\mathbf{y}$ is

$$\mathrm{div}\;\mathbf{f}(\mathbf{x}) = \frac{1}{\sqrt{\widetilde{\tau}_\Omega}}\mathrm{div}_{\mathbf{y}}\left(\mathbf{M}_\Omega{}^{1/2}\,\mathbf{f}\left(\sqrt{\widetilde{\tau}_\Omega}\mathbf{M}_\Omega{}^{-1/2}\mathbf{y}-\mathbf{M}_\Omega{}^{-1}\mathbf{b}_\Omega\right)\right).$$

Considering the expression of the displacement field $\boldsymbol{\xi}^{\boldsymbol{\theta}}:\mathbb{R}^N\to\mathbb{R}^N$ as $\boldsymbol{\xi}^{\boldsymbol{\theta}}(\mathbf{x}) = \boldsymbol{\Xi}_{\Omega,\boldsymbol{\theta}}\,\mathbf{x}+\mathbf{r}_{\Omega,\boldsymbol{\theta}}$, where $\boldsymbol{\Xi}_{\Omega,\boldsymbol{\theta}}$ and $\mathbf{r}_{\Omega,\boldsymbol{\theta}}$ are defined in (2.12) and (2.13), we get

$$
\begin{aligned}
\frac{\mathrm{d}}{\mathrm{d}\Omega}\left[\Phi\left(\Omega\right)\right](\boldsymbol{\theta}) &= \int_{\mathcal{E}(\Psi_\Omega,\tau)} \operatorname{div}\left(f(\mathbf{x})\,\boldsymbol{\xi}^{\boldsymbol{\theta}}(\mathbf{x})\right)\mathrm{d}\mathbf{x} = \int_{\mathcal{E}(\Psi_\Omega,\tau)} \operatorname{div}\left(f(\mathbf{x})\,\left(\boldsymbol{\Xi}_{\Omega,\boldsymbol{\theta}}\,\mathbf{x} + \mathbf{r}_{\Omega,\boldsymbol{\theta}}\right)\right)\mathrm{d}\mathbf{x} \\
&= \sqrt{\frac{\widetilde{\tau}_\Omega^N}{\det \mathbf{M}_\Omega}} \int_{\mathbb{B}_N} \operatorname{div}_{\mathbf{y}}\left(\left(f\left(\sqrt{\widetilde{\tau}_\Omega}\mathbf{M}_\Omega{}^{-1/2}\mathbf{y} - \mathbf{M}_\Omega{}^{-1}\mathbf{b}_\Omega\right)\right.\right. \\
&\qquad \left.\left.\times \mathbf{M}_\Omega{}^{1/2}\left(\boldsymbol{\Xi}_{\Omega,\boldsymbol{\theta}}\mathbf{M}_\Omega{}^{-1/2}\mathbf{y} + \frac{1}{\sqrt{\widetilde{\tau}_\Omega}}\left(\mathbf{r}_{\Omega,\boldsymbol{\theta}} - \boldsymbol{\Xi}_{\Omega,\boldsymbol{\theta}}\mathbf{M}_\Omega{}^{-1}\mathbf{b}_\Omega\right)\right)\right)\right)\mathrm{d}\mathbf{y}.
\end{aligned}
\tag{2.19}
$$

Observing that the normal vector on the unit sphere $\mathbb{S}_{N-1}$ in any point $\mathbf{s}$ coincides with the vector $\mathbf{s}$ itself, (2.19) can be written as an integral on the sphere $\partial\mathbb{B}_N$ according to (2.18). ■

The expression of the derivative of $\Phi(\cdot)$ as found in Proposition 2.2 is valid only if the random vector $\mathbf{X}$ admits a $\mathcal{C}^1$ density function $f(\cdot)$ in an open neighborhood of the ellipsoid $\mathcal{E}(\Psi_\Omega,\tau)$. However, if the sensitivity of $\Phi(\cdot)$ is computed as part of a shape optimization procedure, such assumption should be verified for all shapes obtained during the execution of the algorithm. Therefore, it is crucial that the density $f(\cdot)$ is $\mathcal{C}^1$ in an open subset of $\mathbb{R}^N$ containing all the ellipsoids corresponding to $\Omega_0,\dots,\Omega_{n_{\max}}$. Such condition might be unrealistic if the density $f(\cdot)$ is not $\mathcal{C}^1$ on the entire space $\mathbb{R}^N$ which especially happens if it is compactly supported like the uniform distribution.

The expression (2.18) can be reformulated in order to highlight the terms depending on the argument of the shape derivative $\boldsymbol{\theta}$. We denote $\{\mathbf{e}_1,\dots,\mathbf{e}_N\}$ the canonical basis of $\mathbb{R}^N$, and we consider a basis $\left\{\mathbf{B}^{i,j}\right\}_{0\le i\le j\le N}$ for the space of $N\times N$ symmetric matrices such that

$$
\left[\mathbf{B}^{i,j}\right]_{k,\ell} = \begin{cases} \beta_{i,j}, & \text{if } k=i,\ \ell=j,\\ \beta_{i,j}, & \text{if } k=j,\ \ell=i,\\ 0, & \text{otherwise,}\end{cases} \qquad \beta_{i,j} = \begin{cases} 1, & \text{if } i=j,\\ 1/\sqrt{2}, & \text{if } i\neq j.\end{cases}
$$

Thus, the shape derivative of $\Phi(\cdot)$ in Ω becomes

$$
\begin{aligned}
\frac{\mathrm{d}}{\mathrm{d}\Omega}\left[\Phi\left(\Omega\right)\right](\boldsymbol{\theta}) &= \sum_{1\le i\le j\le N}\left(\left(\mathbf{M}_\Omega{}^{1/2}\boldsymbol{\Xi}_{\Omega,\boldsymbol{\theta}}\mathbf{M}_\Omega{}^{-1/2}\right) : \mathbf{B}^{i,j}\right. \\
&\qquad \left.\times \int_{\mathbb{S}_{N-1}} \sqrt{\frac{\widetilde{\tau}_\Omega^N}{\det\mathbf{M}_\Omega}}\, f\left(\sqrt{\widetilde{\tau}_\Omega}\mathbf{M}_\Omega{}^{-1/2}\mathbf{y} - \mathbf{M}_\Omega{}^{-1}\mathbf{b}_\Omega\right) s_i s_j\,\mathrm{d}\mathbf{s}\right) \\
&+ \sum_{k=1}^{N}\left(\left(\mathbf{r}_{\Omega,\boldsymbol{\theta}} - \boldsymbol{\Xi}_{\Omega,\boldsymbol{\theta}}\mathbf{M}_\Omega{}^{-1}\mathbf{b}_\Omega\right)\cdot\mathbf{e}_k \int_{\mathbb{S}_{N-1}} \sqrt{\frac{\widetilde{\tau}_\Omega^{N-1}}{\det\mathbf{M}_\Omega}}\, f\left(\sqrt{\widetilde{\tau}_\Omega}\mathbf{M}_\Omega{}^{-1/2}\mathbf{y} - \mathbf{M}_\Omega{}^{-1}\mathbf{b}_\Omega\right) s_k\,\mathrm{d}\mathbf{s}\right).
\end{aligned}
\tag{2.20}
$$

The expression (2.20) of the shape derivative of $\Phi(\Omega)$ requires the computation of all the entries of $\boldsymbol{\Xi}_{\Omega,\boldsymbol{\theta}}$ and $\mathbf{r}_{\Omega,\boldsymbol{\theta}}$ (which are functions of $\frac{\mathrm{d}}{\mathrm{d}\Omega}[\mathbf{M}_\Omega](\boldsymbol{\theta})$, $\frac{\mathrm{d}}{\mathrm{d}\Omega}[\mathbf{b}_\Omega](\boldsymbol{\theta})$, and $\frac{\mathrm{d}}{\mathrm{d}\Omega}[c_\Omega](\boldsymbol{\theta})$), as well as $N(N+3)/2$ integrals on $\mathbb{S}_{N-1}$. The evaluation of said integrals can be done by applying suitable quadrature formulas on $\mathbb{S}_{N-1}$, which of course might be quite expensive if the number N of random variables is large. An alternative approach which applies to Gaussian random fields is proposed in the next section.

3. The generalized noncentral chi-squared distribution.

3.1. Series expansion of the cumulative distribution function. Let $\mathbf{X} \sim \mathcal{N}(\boldsymbol{\mu}, \Sigma)$ be a Gaussian random vector with N components, mean $\boldsymbol{\mu}$ and covariance matrix Σ, and let $\mathbf{D} = \operatorname{diag}\{\lambda_1, \ldots, \lambda_N\}$ be a positive definite diagonal matrix. Let T be the random variable defined as follows:

$$T = \mathbf{X}^{\mathrm{T}}\, \mathbf{D}\, \mathbf{X} = \lambda_1 X_1^2 + \ldots + \lambda_N X_N^2, \tag{3.1}$$

Without loss of generality, we suppose that the covariance matrix of the Gaussian random vector $\mathbf{X}$ is the identity matrix: $\mathbf{X} \sim \mathcal{N}(\boldsymbol{\mu}, \mathbb{I})$. In such case, each random variable X_i^2 follows a noncentral chi-squared distribution with one degree of freedom and non-centrality parameter μ_i^2. The random variable T is said to follow a generalized non-central chi-squared distribution:

$$T \sim \widetilde{\chi^2}\left(\mathbf{1}; \boldsymbol{\mu} \odot \boldsymbol{\mu}; \boldsymbol{\lambda}\right), \tag{3.2}$$

where $\mathbf{1} = [1, \ldots, 1]$ is the vector of the degrees of freedom, $\boldsymbol{\mu} \odot \boldsymbol{\mu} = [\mu_1^2, \ldots, \mu_N^2]$ is the vector of noncentrality parameters (the symbol "$\odot$" represent the elementwise product), and $\boldsymbol{\lambda} = \operatorname{diag}\{\mathbf{D}\}$ is the vector of the weights of the random variables $X_1, \ldots, X_N$.

The characterization of the cumulative distribution function F_T of the random variable T has been studied analytically in [36, 37]. The results of these articles have led to the development of several algorithms for the numerical computation of the quantiles of T. Sequential methods that provide an estimate for the truncation error include the algorithms developed by Imhof [28], Farebrother [22] (this method refines the result obtained by Sheil and O'Muircheartaigh in [41]), and Davies [17, 18]. If the number N of random variables is large, faster but less accurate approximations should be considered. Among such techniques we mention Kuonen's method [29], which is based on a saddlepoint approximation of the distribution of T, the approach based on the leading eigenvalues developed by Lumley et al. in [33], and the several approaches based on the computation of the stochastic moments of the random variable T like the methods deveolped by Liu–Tang–Zhang [32], Satterthwaite–Welch [39], Hall-Buckley–Eagleson [25, 5], and Lindsay–Pilla–Basak [31]. Further information on the comparison between the different methods can be found in [20, 4, 8].

In this section, we present the results of [37], where, for any threshold $\tau > 0$, the quantity $F_T(\tau)$ is expressed in terms of a series of cumulative distribution functions of centered chi-squared random variables (see [37, Theorem 1]). The coefficients of the decomposition are defined by a recurrence relation. Moreover, an upper bound on the truncation error of the series is provided.

Theorem 3.1 (Decomposition of $F_T(\tau)$ by chi-squared random variables). *Let T be a real-valued random variable defined as in (3.1). Then, for any choice of $\beta > 0$, the quantity $F_T(\tau) = \mathbb{P}[T \leq \tau]$ can be expressed as*

$$F_T(\tau) = \sum_{k=0}^{\infty} \gamma_k F_{\chi^2(2k+N)}\left(\frac{\tau}{\beta}\right). \tag{3.3}$$

The weights $\{\gamma_k\}_{k=0}^{\infty}$ *are computed by using the recurrence relation*

$$\gamma_0 = e^{-\frac{1}{2}\|\boldsymbol{\mu}\|^2}\beta^{N/2}\det(\mathbf{D})^{-1/2} \quad \text{and} \quad \gamma_k = \frac{1}{2k}\sum_{\ell=0}^{k-1} g_{k-\ell}\gamma_\ell \text{ for } k \geq 1, \tag{3.4}$$

where the coefficients $\{g_k\}_{k=1}^{\infty}$ *are defined in accordance with*

$$g_k = \sum_{i=1}^{N}\left(1-\frac{\beta}{\lambda_i}\right)^{k-1}\left(1+(k\mu_i^2-1)\frac{\beta}{\lambda_i}\right). \tag{3.5}$$

In particular, if $0 < \beta < \min_{i\in\{1,\dots,N\}}\{\lambda_1,\dots,\lambda_N\}$*, the series* (3.3) *is a mixture representation, meaning that all coefficients* γ_k *are non-negative and* $\sum_{k=0}^{\infty}\gamma_k = 1$*.*

This result is stated and proven in [37, Theorem 1], while the condition of the mixture representation is stated in [37, Section 5]. Note that [37] provides also an explicit expression for the coefficients $\{\gamma_k\}_{k=0}^{\infty}$ which can be used to prove the uniform convergence of the series (3.3) for any choice of $\beta > 0$ and for any finite value of the threshold $0 \leq \tau < \infty$. Especially, analogous results apply also to the probability density function of T.

Corollary 3.2. *If* $0 < \beta < \min_{i\in\{1,\dots,N\}}\{\lambda_1,\dots,\lambda_N\}$*, for any* $\tau > 0$*, the following expression for the probability density function of* T *holds:*

$$f_T(\tau) = \sum_{k=0}^{\infty}\gamma_k f_{\chi^2(2k+N)}\left(\frac{\tau}{\beta}\right).$$

If the mixture representation holds (that is if $0 < \beta < \min\{\lambda_1,\dots,\lambda_N\}$), it is possible to establish the following upper bound on the truncation error of the series (3.3).

Proposition 3.3. *If* $0 < \beta < \min\{\lambda_1,\dots,\lambda_N\}$ *and the hypotheses of Theorem 3.1 hold, then*

$$\left|F_T(\tau) - \sum_{k=0}^{n}\gamma_k F_{\chi^2(2k+N)}\left(\frac{\tau}{\beta}\right)\right| \leq \left(1-\sum_{k=0}^{n}\gamma_k\right)F_{\chi^2(2n+2+N)}\left(\frac{\tau}{\beta}\right) \tag{3.6}$$

for all $0 < \tau < \infty$ *and any integer* n*.*

Proof. One readily verifies that $F_{\chi^2(m)}(\tau) < F_{\chi^2(n)}(\tau)$ for any pair of integers $m > n$ and any $\tau > 0$ fixed. Therefore, the sequence $\left\{F_{\chi^2(2k+N+2)}\left(\frac{\tau}{\beta}\right)\right\}_{k=0}^{\infty}$ is decreasing whenever τ/β is fixed. Thus, we conclude

$$\begin{aligned}\left|F_T(\tau) - \sum_{k=0}^{n}\gamma_k F_{\chi^2(2k+N)}\left(\frac{\tau}{\beta}\right)\right| &= \left|\sum_{k=n+1}^{\infty}\gamma_k F_{\chi^2(2k+N)}\left(\frac{\tau}{\beta}\right)\right| \\ &\leq F_{\chi^2(2n+N+2)}\left(\frac{\tau}{\beta}\right)\sum_{k=n+1}^{\infty}\gamma_k = \left(1-\sum_{k=0}^{n}\gamma_k\right)F_{\chi^2(2n+2+N)}\left(\frac{\tau}{\beta}\right). \quad \blacksquare\end{aligned}$$

3.2. Differentiating the probability of a quadratic form to exceed a threshold. Let τ be a positive constant, and let us consider the following mappings:

- $\mathbf{M} : [0,\delta] \to \mathrm{Sym}_N$ associating to any $t \in [0,\delta]$ a positive definite symmetric matrix;
- $\mathbf{b} : [0,\delta] \to \mathbb{R}^N$;
- $c : [0,\delta] \to \mathbb{R}$.

We assume that these three functions are all $\mathcal{C}^1$, and we denote by Ψ_t the quadratic form defined on $\mathbb{R}^N$ given by

$$\Psi_t : \mathbf{x} \mapsto \mathbf{x}^{\mathrm{T}}\mathbf{M}(t)\mathbf{x} + 2^{\mathrm{T}}\mathbf{b}(t)\mathbf{x} + c(t). \tag{3.7}$$

We suppose that $\Psi_t(\mathbf{x}) > 0$ and that $\tau > c(t) - \mathbf{b}^{\mathrm{T}}(t)\mathbf{M}^{-1}(t)\mathbf{b}(t) = \Psi_t\left(-\mathbf{M}^{-1}(t)\mathbf{b}(t)\right)$ holds for all $t \in [0,\delta]$ and $\mathbf{x} \in \mathbb{R}^N$.

Let $\mathbf{X} \sim \mathcal{N}(\mathbf{h}, \mathbb{I})$ be a Gaussian random vector where $\mathbf{h} \in \mathbb{R}^N$ is constant and $\mathbb{I}$ is the $N \times N$ identity matrix. We are interested in differentiating the cumulative distribution function of the random variable $\Psi_t(\mathbf{X})$ with respect to the parameter t. In order to do so, we prove the following lemma about the derivative of the cumulative distribution function of a generalized $\widetilde{\chi^2}$ random variable.

Lemma 3.4. *Let us consider two $\mathcal{C}^1$ vector-valued functions $\boldsymbol{\mu}, \boldsymbol{\lambda} : [0,\delta] \to \mathbb{R}^N$ such that, for all $t \in [0,\delta]$, all components of $\boldsymbol{\lambda}(t)$ are strictly larger than a positive constant β independent from t. For all $t \in [0,\delta]$, let $T(t)$ be a random variable with the following generalized chi-squared distribution:*

$$T(t) \sim \widetilde{\chi^2}\left(\mathbf{1}; \boldsymbol{\mu}(t) \odot \boldsymbol{\mu}(t); \boldsymbol{\lambda}(t)\right), \tag{3.8}$$

Due to Theorem 3.1, its cumulative distribution function evaluated in τ can be expressed as

$$F_{T(t)}(\tau) = \sum_{k=0}^{\infty} \gamma_k(t) F_{\chi^2(2k+N)}\left(\frac{\tau}{\beta}\right). \tag{3.9}$$

Then, the coefficients $\gamma_k(t)$ of the respective cumulative distribution function (3.3) evaluated in τ are differentiable with respect to t for all $t \in [0,\delta]$ and all $k \in \mathbb{N}$, and their derivative is

$$\gamma_k'(t) = \boldsymbol{\lambda}'(t) \cdot \mathbf{p}^k + \boldsymbol{\mu}'(t) \cdot \mathbf{q}^k.$$

Herein, the terms $\mathbf{p}^k = [p_1^k, \dots, p_N^k]^{\mathrm{T}}$ and $\mathbf{q}^k = [q_1^k, \dots, q_N^k]^{\mathrm{T}}$, and $\mathbf{d}^j$ are defined as follows for any $j \in \{1, \dots, N\}$ and $k \geq 0$:

- $p_j^0 = -\frac{\gamma_0}{2\lambda_j}$ *and* $p_j^k = \frac{1}{2k}\sum_{\ell=0}^{k-1}\left(\nu_j^{k-\ell}\gamma_\ell + p_j^\ell g_{k-\ell}\right)$ *for* $k \geq 1$*;*
- $q_j^0 = 0$ *and* $q_j^k = \frac{1}{2k}\sum_{\ell=0}^{k-1}\left(\kappa_j^{k-\ell}\gamma_\ell + q_j^\ell g_{k-\ell}\right)$ *for* $k \geq 1$*;*
- $\nu_j^1 = \frac{\beta}{\lambda_j^2}\left(1-\mu_j^2\right)$ *and* $\nu_j^k = \frac{\beta}{\lambda_j^2}\left(1-\frac{\beta}{\lambda_j}\right)^{k-2}\left[(k-1)\left(1+\frac{\beta}{\lambda_j}(k\mu_j^2-1)\right) + \left(1-\frac{\beta}{\lambda_j}\right)(1-k\mu_j^2)\right]$ *for* $k \geq 1$*;*
- $\kappa_j^k = 2k\mu_j\frac{\beta}{\lambda_j}\left(1-\frac{\beta}{\lambda_j}\right)^{k-1}$ *for* $k \geq 1$*.*

Proof. According to Theorem 3.1, the coefficients γ_k are defined as in (3.4), where the coefficients g_k are given by:

$$g_k = \sum_{j=1}^{N}\left(1-\frac{\beta}{\lambda_j}\right)^{k-1}\left(1+(k\mu_j(t)^2-1)\frac{\beta}{\lambda_j(t)}\right). \tag{3.10}$$

Differentiating (3.10), we obtain

$$g_1'(t) = \sum_{j=1}^{N} \left(2\frac{h_i\beta}{\lambda_j}\mu_j'(t) - (h_j^2 - 1)\frac{\beta}{\lambda_j^2}\lambda_j'(t) \right) = \sum_{j=1}^{N} \left(\kappa_j^1 \mu_j'(t) + \nu_j^1 \lambda_j'(t) \right)$$

and for $k > 1$

$$\begin{aligned} g_k'(t) = \sum_{j=1}^{N} \Bigg[&\left(1 - \frac{\beta}{\lambda_j}\right)^{k-2} \left((k-1)\frac{\beta}{\lambda_j^2} \left(1 + (k\mu_j^2 - 1)\frac{\beta}{\lambda_j} \right) \right) \lambda_j'(t) \\ &+ \left(1 - \frac{\beta}{\lambda_j}\right) \left(2k\frac{\mu_j\beta}{\lambda_j}\mu_j'(t) - \left((k\mu_j^2 - 1)\frac{\beta}{\lambda_j(t)^2} \right) \lambda_j'(t) \right) \Bigg] = \sum_{j=1}^{N} \left(\kappa_j^k \mu_j'(t) + \nu_j^k \lambda_j'(t) \right). \end{aligned}$$

The assertion follows by differentiating the definitions of γ_k, found in (3.4), and using the expression above for the derivatives of g_k. ■

Proposition 3.5. *Let $\Psi_t : \mathbb{R}^N \to \mathbb{R}$ be defined as in (3.7) for $t \in [0, \delta]$, let $\mathbf{X} \sim \mathcal{N}(\mathbf{h}, \mathbb{I})$ be a Gaussian vector, and let τ be a positive constant. We assume that $\tau > c(t) - \mathbf{b}^{\mathrm{T}}(t)\mathbf{M}^{-1}(t)\mathbf{b}(t)$ for all $t \in [0, \delta]$, and that all eigenvalues of $\mathbf{M}(t)$ $\lambda_1(t), \ldots, \lambda_N(t)$ are pairwise distinct and larger than a strictly positive constant $\beta > 0$. We introduce the following notation:*

- *$\mathbf{Y}(t) \in \mathrm{L}^2(\mathcal{O}, \mathbb{P})$ is the random variable defined as $\mathbf{Y}(t) = \mathbf{X} + \mathbf{M}^{-1}(t)\mathbf{b}(t)$, therefore its law is $\mathbf{Y}(t) \sim \mathcal{N}\left(\mathbf{h} + \mathbf{M}^{-1}(t)\mathbf{b}(t), \mathbb{I}\right)$;*
- *for all $t \in [0, \delta]$, we denote $T(t)$ the random variable $T(t) = \mathbf{Y}^{\mathrm{T}}(t)\mathbf{M}(t)\mathbf{Y}(t)$;*
- *$\widetilde{\tau} : [0, \delta] \to \mathbb{R}$ mapping $t \mapsto \tau - c(t) + \mathbf{b}(t)^{\mathrm{T}}\mathbf{M}^{-1}(t) + \mathbf{b}(t)$;*
- *$\mathbf{M}(t)$ is diagonalized as $\mathbf{M}(t) = \mathbf{Q}(t)\mathbf{D}(t)\mathbf{Q}^{\mathrm{T}}(t)$, where $\mathbf{Q}(t) = [\mathbf{v}^1|, \ldots, |\mathbf{v}^N]$ is an orthogonal matrix, and $\mathbf{D}(t) = \operatorname{diag}\{\boldsymbol{\lambda}(t)\} = \operatorname{diag}\{\lambda_1(t), \ldots, \lambda_N(t)\}$;*
- *$\boldsymbol{\mu} : [0, \delta] \to \mathbb{R}^N$ such that $\boldsymbol{\mu}(t) = \mathbf{Q}^{\mathrm{T}}(t)\mathbf{h} + \mathbf{Q}^{\mathrm{T}}(t)\mathbf{M}^{-1}(t)\mathbf{b}(t)$.*

Then, for any $t \in [0, \delta]$, $\mathbf{Y}(t)$ is a normalized Gaussian random variable centered in $\boldsymbol{\mu}(t)$, and $T(t)$ has the following chi-squared distribution:

$$T(t) \sim \widetilde{\chi^2}\left(\mathbf{1}; \boldsymbol{\mu}(t) \odot \boldsymbol{\mu}(t); \boldsymbol{\lambda}\right). \tag{3.11}$$

Moreover, for all $t \in [0, \delta]$, the following identity between the values of the cumulative distribution functions of $\Psi_t(\mathbf{X})$ and $T(t)$ holds:

$$F_{\Psi_t(\mathbf{X})}(\tau) = F_{T(t)}(\widetilde{\tau}(t)). \tag{3.12}$$

Finally, the mapping $t \mapsto F_{\Psi_t(\mathbf{X})}(\tau)$ is differentiable and its derivative can be written as

$$\begin{aligned} \frac{\mathrm{d}}{\mathrm{d}t} F_{\Psi_t(\mathbf{X})}(\tau) = &\left(\sum_{k=0}^{\infty} \mathbf{p}^k F_{\chi^2(2k+N)}\left(\frac{\widetilde{\tau}(t)}{\beta} \right) \right) \cdot \boldsymbol{\lambda}'(t) \\ &+ \left(\sum_{k=0}^{\infty} \mathbf{q}^k F_{\chi^2(2k+N)}\left(\frac{\widetilde{\tau}(t)}{\beta} \right) \right) \cdot \boldsymbol{\mu}'(t) + \frac{1}{\beta} \left(\sum_{k=0}^{\infty} \gamma_k f_{\chi^2(2k+N)}\left(\frac{\widetilde{\tau}(t)}{\beta} \right) \right) \widetilde{\tau}'(t). \end{aligned} \tag{3.13}$$

Here, for all $n \in \mathbb{N}$, $f_{\chi^2(n)}$ is the density of a chi-squared random variable with n degrees of freedom. The components of $\mathbf{p}^k$ and $\mathbf{q}^k$ are the coefficients appearing in the decomposition of $F_{T(t)}\left(\widetilde{\tau}(t)\right)$ expressed as in Lemma 3.4, while the derivatives of $\boldsymbol{\lambda}$, $\boldsymbol{\mu}$, and $\widetilde{\tau}$ are:

$$\boldsymbol{\lambda}'(t) = \operatorname{diag}\left\{\mathbf{Q}^{\mathrm{T}}(t)\mathbf{M}'(t)\mathbf{Q}(t)\right\}; \tag{3.14}$$

$$\begin{aligned}\mu_i'(t) = \sum_{j\neq i}\left(\frac{1}{\lambda_i-\lambda_i}\left({\mathbf{v}^i}^{\mathrm{T}}\mathbf{M}'(t)\mathbf{v}^j\right)\left({\mathbf{v}^j}^{\mathrm{T}}\left(\mathbf{h}+\mathbf{M}^{-1}(t)\mathbf{b}(t)\right)\right)\right)\\ + {\mathbf{v}^i}^{\mathrm{T}}\left(\mathbf{M}^{-1}(t)\mathbf{b}'(t)+\mathbf{M}^{-1}(t)\mathbf{M}'(t)\mathbf{M}^{-1}(t)\mathbf{b}(t)\right) \quad \textit{for all } i\in\{1,\dots,N\};\end{aligned} \tag{3.15}$$

$$\widetilde{\tau}'(t) = -\frac{\mathrm{d}}{\mathrm{d}t}c(t) - \mathbf{b}^{\mathrm{T}}(t)\mathbf{M}^{-1}(t)\mathbf{M}'(t)\mathbf{M}^{-1}(t)\mathbf{b}(t) + 2\mathbf{b}^{\mathrm{T}}(t)\mathbf{M}^{-1}(t)\mathbf{b}'(t). \tag{3.16}$$

Proof. The identity (3.12) follows from

$$\begin{aligned}F_{\Psi_t(\mathbf{X})}(\tau) &= \mathbb{P}\left[\Psi_t(\mathbf{X})\le\tau\right] = \mathbb{P}\left[\mathbf{X}^{\mathrm{T}}\mathbf{M}(t)\mathbf{X}+2\mathbf{b}(t)^{\mathrm{T}}\mathbf{X}+c(t)\le\tau\right]\\ &= \mathbb{P}\left[\left(\mathbf{X}+\mathbf{M}^{-1}(t)\mathbf{b}(t)\right)^{\mathrm{T}}\mathbf{M}(t)\left(\mathbf{X}+\mathbf{M}^{-1}(t)\mathbf{b}(t)\right)\le\tau-c(t)+\mathbf{b}(t)^{\mathrm{T}}\mathbf{M}^{-1}(t)+\mathbf{b}(t)\right]\\ &= \mathbb{P}\left[T(t)\le\widetilde{\tau}(t)\right] = F_{T(t)}\left(\widetilde{\tau}(t)\right).\end{aligned}$$

We prove next the differentiability of $\boldsymbol{\lambda}$, $\boldsymbol{\mu}$, and $\widetilde{\tau}$ and equations (3.14), (3.15), and (3.16). Equation (3.14) can be deduced directly from [34, Equation (4)]. Equation (3.15) can be proven by using [34, Equation (5)] on the derivative of the eigenvector of a symmetric matrix with distinct eigenvalues

$${\mathbf{v}^i}'(t) = \left(\lambda_i\mathbb{I}-\mathbf{M}(t)\right)^{+}\mathbf{M}'(t)\mathbf{v}^i(t) = \sum_{j\neq i}\frac{1}{\lambda_i-\lambda_j}\left({\mathbf{v}^j}^{\mathrm{T}}\mathbf{M}'(t)\mathbf{v}^i\right)\mathbf{v}^j,$$

where the symbol "+" denotes the Moore-Penrose inverse. Indeed, using the properties of the Moore-Penrose inverse, we arrive at

$$\left(\lambda_i\mathbb{I}-\mathbf{M}\right)^{+} = \left(\mathbf{Q}\left(\lambda_i\mathbb{I}-\mathbf{D}\right)\mathbf{Q}^{\mathrm{T}}\right)^{+} = \mathbf{Q}(t)\operatorname{diag}\left\{\mathbf{d}^i(t)\right\}\mathbf{Q}(t)^{\mathrm{T}}.$$

Herein, for all $i,j\in\{1,\dots,N\}$, $\mathbf{d}^i(t) = [d_1^i(t),\dots,d_N^i(t)]^{\mathrm{T}}$ with $d_i^i = 0$ and $d_j^i = \frac{1}{\lambda_i(t)-\lambda_j(t)}$ if $i\neq j$. Since $\mu_i(t) = {\mathbf{v}^i}^{\mathrm{T}}\mathbf{M}^{-1}(t)\mathbf{b}(t)$ for all $1\le i\le N$, we deduce

$$\mu_i'(t) = {\mathbf{v}^i}'(t)^{\mathrm{T}}\mathbf{M}^{-1}(t)\mathbf{b}(t) + \mathbf{v}^i(t)^{\mathrm{T}}\mathbf{M}^{-1}(t)\mathbf{M}'(t)\mathbf{M}^{-1}(t)\mathbf{b}(t)\mathbf{M}^{-1}(t)\mathbf{b}'(t),$$

which is equivalent to (3.15). Next, Equation (3.16) can be computed directly applying the chain rule on the definition (3.16) of $\widetilde{\tau}$.

Finally, in order to prove the expression (3.13) of the derivative of $F_{\Psi_t(T)}(\tau)$, we consider the identity (3.12) and the result of Theorem 3.1 to write

$$F_{\Psi_t(\mathbf{X})}(\tau) = F_{T(t)}\left(\widetilde{\tau}(t)\right) = \sum_{k=0}^{\infty}\gamma_k(t)F_{\chi^2(2k+N)}\left(\frac{\widetilde{\tau}(t)}{\beta}\right).$$

By differentiating both sides with respect to t, we obtain

$$\frac{\mathrm{d}}{\mathrm{d}t} F_{\Psi_t(\mathbf{X})}(\tau) = \frac{\partial}{\partial t_1} F_{T(t_1)}(\widetilde{\tau}(t))\bigg|_{t_1=t} + \frac{\partial}{\partial t_2} F_{T(t)}(\widetilde{\tau}(t_2))\bigg|_{t_2=t}. \tag{3.17}$$

We treat the two terms on the right-hand side of (3.17) separately.

In order to evaluate the first term, we aim to prove the uniform convergence of the series $\sum_{k=0}^{\infty} \mathbf{p}^k \cdot \boldsymbol{\lambda}'(t) F_{\chi^2(2k+N)}\left(\frac{\widetilde{\tau}(t)}{\beta}\right)$ and $\sum_{k=0}^{\infty} \mathbf{q}^k \cdot \boldsymbol{\mu}'(t) F_{\chi^2(2k+N)}\left(\frac{\widetilde{\tau}(t)}{\beta}\right)$. We start proving by induction the inequalities

$$\left|p_j^k\right| \leq \eta_k \gamma_k \qquad \text{and} \qquad \left|q_j^k\right| \leq \zeta_k \gamma_k \text{ for all } j \in \{1,\dots,N\},\ k \geq 0, \tag{3.18}$$

where η_k and ζ_k are defined for $k \geq 0$ as

$$\begin{aligned} \eta_k &= \max_{1\leq i\leq N}\left\{\frac{1}{2\lambda_i}\right\} + \frac{k(k+1)}{2} \max_{1\leq i\leq N}\left\{\frac{\beta(h_i^2+3)}{\lambda_i^2\left(1-\frac{\beta}{\lambda_i}\right)}\right\}, \\ \zeta_k &= \frac{k(k+1)}{2} \max_{1\leq i\leq N}\left\{\frac{2\beta\left|h_i\right|}{\lambda_i^2\left(1-\frac{\beta}{\lambda_i}\right)}\right\}. \end{aligned} \tag{3.19}$$

For $k = 0$, the inequalities in (3.18) are satisfied. Let us therefore suppose that they are valid for the step $k-1$ and prove that they hold for the step k. Thanks to the fact that $0 < \beta < \min_{i\in\{1,\dots,N\}}\{\lambda_1,\dots,\lambda_N\}$, we have for all $k \geq 1$ that

$$\begin{aligned} \left|\nu_j^k\right| &\leq \frac{\beta}{\lambda_j^2}\frac{(k-1)}{\left(1-\frac{\beta}{\lambda_j}\right)}\left(1-\frac{\beta}{\lambda_j}\right)^{k-1}\left(1+(kh_j^2-1)\frac{\beta}{\lambda_j^2}\right) + \frac{\beta}{\lambda_j^2}\left(1-\frac{\beta}{\lambda_j}\right)^{k-1}\left|kh_j^2-1\right| \\ &\leq \frac{\beta}{\lambda_j^2} g_k \left(\frac{k-1}{\left(1-\frac{\beta}{\lambda_j}\right)} + \frac{\left|kh_j^2-1\right|}{\left(1-\frac{\beta}{\lambda_j}+\frac{\beta}{\lambda_j}kh_j^2\right)}\right) \leq \frac{\beta}{\lambda_j^2} g_k \frac{k-1+\left|1-kh_j^2\right|}{\left(1-\frac{\beta}{\lambda_j}\right)} \\ &\leq k g_k \beta \max_{i\in\{1,\dots,N\}}\left\{\frac{1+h_j^2+2/k}{\lambda_j^2\left(1-\frac{\beta}{\lambda_j}\right)}\right\} \leq k g_k \max_{i\in\{1,\dots,N\}}\left\{\frac{\beta(h_j^2+3)}{\lambda_j^2\left(1-\frac{\beta}{\lambda_j}\right)}\right\} \end{aligned}$$

and

$$\begin{aligned} \left|\kappa_j^k\right| &\leq 2k\left|h_j\right|\frac{\beta}{\lambda_j}\left(1-\frac{\beta}{\lambda_j}\right)^{k-1}\frac{\left(1+(kh_j^2-1)\frac{\beta}{\lambda_j^2}\right)}{\left(1-\frac{\beta}{\lambda_j^2}+kh_j^2\frac{\beta}{\lambda_j^2}\right)} \\ &\leq \frac{2kg_k\left|h_j\right|\beta}{\lambda_j\left(1-\frac{\beta}{\lambda_j}\right)} \leq k g_k \max_{i\in\{1,\dots,N\}}\left\{\frac{2\beta\left|h_j\right|}{\lambda_j\left(1-\frac{\beta}{\lambda_j}\right)}\right\}. \end{aligned}$$

In view of such upper bounds and since the sequences $\{\eta_k\}_{k=0}^{\infty}$ and $\{\zeta_k\}_{k=0}^{\infty}$ defined in (3.19) are strictly increasing, we arrive at

$$\begin{aligned}
\left|p_j^k\right| &= \left|\frac{1}{2k}\sum_{\ell=0}^{k-1}\left(\nu_j^{k-\ell}\gamma_\ell + p_j^\ell g_{k-\ell}\right)\right| \le \frac{1}{2k}\sum_{\ell=0}^{k-1}\left|\nu_j^{k-\ell}\right|\gamma_\ell + \frac{1}{2k}\sum_{\ell=0}^{k-1}\left|p_j^\ell\right| g_{k-\ell} \\
&\le \max_{i\in\{1,\dots,N\}}\left\{\frac{\beta(h_j^2+3)}{\lambda_j^2\left(1-\frac{\beta}{\lambda_j}\right)}\right\}\frac{1}{2k}\sum_{\ell=0}^{k-1}(k-\ell)g_{k-\ell}\gamma_\ell + \frac{1}{2k}\sum_{\ell=0}^{k-1}\eta_\ell\gamma_\ell g_{k-\ell} \\
&\le \max_{i\in\{1,\dots,N\}}\left\{\frac{\beta(h_j^2+3)}{\lambda_j^2\left(1-\frac{\beta}{\lambda_j}\right)}\right\}\frac{k}{2k}\sum_{\ell=0}^{k-1}g_{k-\ell}\gamma_\ell + \frac{1}{2k}\eta_{k-1}\sum_{\ell=0}^{k-1}\gamma_\ell g_{k-\ell} \\
&= \left(k\max_{i\in\{1,\dots,N\}}\left\{\frac{\beta(h_j^2+3)}{\lambda_j^2\left(1-\frac{\beta}{\lambda_j}\right)}\right\} + \eta_{k-1}\right)\gamma_k = \eta_k\,\gamma_k,
\end{aligned}$$

and

$$\begin{aligned}
\left|q_j^k\right| &= \left|\frac{1}{2k}\sum_{\ell=0}^{k-1}\left(\kappa_j^{k-\ell}\gamma_\ell + q_j^\ell g_{k-\ell}\right)\right| \le \frac{1}{2k}\sum_{\ell=0}^{k-1}\left|\kappa_j^{k-\ell}\right|\gamma_\ell + \frac{1}{2k}\sum_{\ell=0}^{k-1}\left|q_j^\ell\right| g_{k-\ell} \\
&\le \max_{i\in\{1,\dots,N\}}\left\{\frac{2\beta\,|h_j|}{\lambda_j\left(1-\frac{\beta}{\lambda_j}\right)}\right\}\frac{1}{2k}\sum_{\ell=0}^{k-1}(k-\ell)g_{k-\ell}\gamma_\ell + \frac{1}{2k}\sum_{\ell=0}^{k-1}\zeta_\ell\gamma_\ell g_{k-\ell} \\
&\le \max_{i\in\{1,\dots,N\}}\left\{\frac{2\beta\,|h_j|}{\lambda_j\left(1-\frac{\beta}{\lambda_j}\right)}\right\}\frac{k}{2k}\sum_{\ell=0}^{k-1}g_{k-\ell}\gamma_\ell + \frac{1}{2k}\zeta_{k-1}\sum_{\ell=0}^{k-1}\gamma_\ell g_{k-\ell} \\
&= \left(k\max_{i\in\{1,\dots,N\}}\left\{\frac{2\beta\,|h_j|}{\lambda_j\left(1-\frac{\beta}{\lambda_j}\right)}\right\} + \zeta_{k-1}\right)\gamma_k = \zeta_k\,\gamma_k.
\end{aligned}$$

In order to prove the uniform convergence of the series of (3.18), we use two results from [37]. The first one is presented as [37, Equation (4.14)] and states that

$$\gamma_k \le \gamma_0\frac{\Gamma\left(\frac{N}{2}+k\right)}{\Gamma\left(\frac{N}{2}\right)}\frac{\nu^k}{k!} \tag{3.20}$$

for any $k \ge 0$, where ν is a positive constant depending on β, $\boldsymbol{\lambda}(t)$, and $\boldsymbol{\mu}(t)$. The second result is [37, Lemma 4] and states that the series

$$\sum_{k=0}^{\infty}\frac{\Gamma\left(\frac{N}{2}+k\right)}{\Gamma\left(\frac{N}{2}\right)}\frac{\widetilde{\nu}^k}{k!}F_{\chi^2(2k+N)}(x) \tag{3.21}$$

is uniformly convergent (and therefore absolutely convergent) for any positive and finite $\widetilde{\nu}$ and $\bar{x}$ on the interval $[-\infty, \bar{x}]$. Thus, we can introduce the quantities ρ_1, ρ_2, σ_1 and σ_2 with the property

$$\eta_k \le \rho_1 \sigma_1^k \qquad \text{and} \qquad \zeta_k \le \rho_2 \sigma_2^k \text{ for all } k \ge 0. \tag{3.22}$$

A suitable choice is given by

$$\begin{aligned} \rho_1 &= \max_{1\le i\le N}\left\{\frac{1}{2\lambda_i}\right\}, & \rho_2 &= 1, \\ \sigma_1 &= \max_{1\le i\le N}\left\{\frac{\beta(h_i^2+3)}{\lambda_i^2\left(1-\frac{\beta}{\lambda_i}\right)}\right\}, & \sigma_2 &= \max_{1\le i\le N}\left\{\frac{2\beta\,|h_i|}{\lambda_i^2\left(1-\frac{\beta}{\lambda_i}\right)}\right\}. \end{aligned} \tag{3.23}$$

Using the bounds from (3.18) and the two results from [37] stated above, we remark that the first and second series in (3.13) are absolutely convergent, since

$$\begin{aligned} \sum_{k=0}^{\infty}\left|p_j^k\right| F_{\chi^2(N+2k)}\left(\frac{\tau}{\beta}\right) &\le \sum_{k=0}^{\infty}\eta_k\gamma_k F_{\chi^2(N+2k)}\left(\frac{\tau}{\beta}\right) \\ &\le \sum_{k=0}^{\infty}\rho_1\gamma_0\frac{\Gamma\left(\frac{N}{2}+k\right)}{\Gamma\left(\frac{N}{2}\right)}\frac{(\sigma_1\nu)^k}{k!}F_{\chi^2(N+2k)}\left(\frac{\tau}{\beta}\right) < \infty, \end{aligned}$$

and

$$\begin{aligned} \sum_{k=0}^{\infty}\left|q_j^k\right| F_{\chi^2(N+2k)}\left(\frac{\tau}{\beta}\right) &\le \sum_{k=0}^{\infty}\zeta_k\gamma_k F_{\chi^2(N+2k)}\left(\frac{\tau}{\beta}\right) \\ &\le \sum_{k=0}^{\infty}\rho_2\gamma_0\frac{\Gamma\left(\frac{N}{2}+k\right)}{\Gamma\left(\frac{N}{2}\right)}\frac{(\sigma_2\nu)^k}{k!}F_{\chi^2(N+2k)}\left(\frac{\tau}{\beta}\right) < \infty. \end{aligned}$$

Thus, the series $\sum_{k=0}^{\infty}\mathbf{p}^k\cdot\boldsymbol{\lambda}'(t)F_{\chi^2(2k+N)}\left(\frac{\widetilde{\tau}(t)}{\beta}\right)$ and $\sum_{k=0}^{\infty}\mathbf{q}^k\cdot\boldsymbol{\mu}'(t)F_{\chi^2(2k+N)}\left(\frac{\widetilde{\tau}(t)}{\beta}\right)$ are absolutely convergent and, hence, uniformly convergent by the Weierstrass criterion (see e.g. [38, Theorem 7.10]). Consequently, it is possible to swap the summation and the derivative for the first term of (3.17) (see [38, Theorem 7.17]) and we obtain

$$\begin{aligned} &\sum_{k=0}^{\infty}\left(\mathbf{p}^k\cdot\boldsymbol{\lambda}'(t)F_{\chi^2(2k+N)}\left(\frac{\widetilde{\tau}(t)}{\beta}\right)\right)+\sum_{k=0}^{\infty}\left(\mathbf{q}^k\cdot\boldsymbol{\mu}'(t)F_{\chi^2(2k+N)}\left(\frac{\widetilde{\tau}(t)}{\beta}\right)\right) \\ &\qquad=\sum_{k=0}^{\infty}\left(\mathbf{p}^k\cdot\boldsymbol{\lambda}'(t)F_{\chi^2(2k+N)}\left(\frac{\widetilde{\tau}(t)}{\beta}\right)+\mathbf{q}^k\cdot\boldsymbol{\mu}'(t)F_{\chi^2(2k+N)}\left(\frac{\widetilde{\tau}(t)}{\beta}\right)\right) \\ &=\sum_{k=0}^{\infty}\gamma_k'(t)F_{\chi^2(2k+N)}\left(\frac{\widetilde{\tau}(t)}{\beta}\right)=\frac{\partial}{\partial t_1}\sum_{k=0}^{\infty}\gamma_k(t)F_{\chi^2(2k+N)}\left(\frac{\widetilde{\tau}(t)}{\beta}\right)=\frac{\partial}{\partial t_1}F_{T(t_1)}\left(\widetilde{\tau}(t)\right)\Big|_{t_1=t}. \end{aligned} \tag{3.24}$$

We pass to the second term of (3.17). Since the generalized chi-squared distribution of $T(t)$ is continuous in $\mathbb{R}^+$, for any $\tau^*>0$ the quantity $f_{T(t)}(\tau^*)$ exists and is finite for any $\tau^*>0$. Moreover, thanks to Theorem 3.1 and Corollary 3.2, $f_{T(t)}(\tau^*)=\sum_{k=0}^{\infty}\gamma_k(t)f_{\chi^2(2k+N)}\left(\frac{\tau^*}{\beta}\right)$.

Since the set $\mathfrak{T} = \{\widetilde{\tau}(t) : t \in [0,\delta]\}$ is compact, the series converges point wise, and all of its terms are positive, the series $\sum_{k=0}^{\infty} \gamma_k(t) f_{\chi^2(2k+N)}\left(\frac{\tau^*}{\beta}\right)$ is uniformly convergent on $\mathfrak{T}$ (see [38, Theorem 7.13]). Hence, thanks to the absolute continuity of $\widetilde{\tau}'(t)$ for all $t \in [0,\delta]$, we have

$$\begin{aligned}(3.25)\quad \frac{\widetilde{\tau}'(t)}{\beta}\sum_{k=0}^{\infty}\gamma_k(t) f_{\chi^2(2k+N)}\left(\frac{\widetilde{\tau}(t)}{\beta}\right) &= \sum_{k=0}^{\infty}\frac{\partial}{\partial t_2}\left(\gamma_k(t) F_{\chi^2(2k+N)}\left(\frac{\widetilde{\tau}(t_2)}{\beta}\right)\right)\Big|_{t_2=t} \\ &= \frac{\partial}{\partial t_2}\left(\sum_{k=0}^{\infty}\gamma_k(t) F_{\chi^2(2k+N)}\left(\frac{\widetilde{\tau}(t_2)}{\beta}\right)\right)\Big|_{t_2=t} = \frac{\partial}{\partial t_2} F_{T(t)}\left(\widetilde{\tau}(t_2)\right)\Big|_{t_2=t}.\end{aligned}$$

In conclusion, the combination of the equations (3.17), (3.24), and (3.25) proves the expression (3.13) for the derivative of the cumulative distribution function of $\Psi_t(\mathbf{X})$. ■

3.3. Shape optimization under Gaussian perturbations. Let us consider once again the shape optimization problem (2.3). Using the notations of Section 2, we suppose that the random vector $\mathbf{X}$ follows a Gaussian distribution with mean $\mathbf{h} = [h_1, \ldots, h_N]^{\mathrm{T}}$ and, without loss of generality, covariance matrix equal to the identity.

If the vector $\mathbf{h}$ or the deterministic load $\mathbf{g}_0$ are large enough, the uncertain component can be seen as a small random perturbation around a deterministic load $\overline{\mathbf{g}} = \mathbf{g}_0 + \overline{\mathbf{g}}_1 h_1 + \ldots + \overline{\mathbf{g}}_N h_N$, and the shape derivative can be computed as in [2, Section 4.2.3]. Otherwise, if the mechanical loads are centered on 0 or the uncertainties are wide enough not to be treated as small perturbations, a different method should be considered. If the probability density $f_{\mathbf{X}}$ of the uncertainties is known, the technique detailed in Subsection 2.3 can be applied. However, if the number of random variables involved in the modelization of the uncertainties is significant, the computation of the integrals on the N-ball and the N-sphere can be challenging.

Since we suppose that $\mathbf{X}$ follows a Gaussian distribution, by considering the diagonalization of the matrix $\mathbf{M}_\Omega = \mathbf{Q}_\Omega \mathbf{D}_\Omega \mathbf{Q}_\Omega^{\mathrm{T}}$, we can use Corollary 3.2 and Proposition 3.5 to express $\Phi(\Omega) = \mathbb{P}[\Psi_\Omega(\mathbf{X}) \le \tau]$ as the cumulative distribution function of a generalized chi-squared random variable, and compute the shape derivative of $\Phi(\cdot)$ in $\Omega \in \mathcal{S}_{adm}$.

Proposition 3.6. *Let $\mathbf{X} \sim \mathcal{N}(\boldsymbol{\mu}, \mathbb{I})$ be a Gaussian random vector in $\mathbb{R}^N$, $\Omega \in \mathcal{S}_{adm}$ a Lipschitz-continuous domain in $\mathbb{R}^2$ or $\mathbb{R}^3$, and $\tau \in \mathbb{R}^+$ a strictly positive threshold. The quantities $\mathbf{M}_\Omega \in \mathrm{Sym}_N$, $\mathbf{b}_\Omega \in \mathbb{R}^N$, and $c_\Omega \in \mathbb{R}$ are functions of the domain $\Omega \in \mathcal{S}_{adm}$, and are defined as in Subsection 2.2, and we suppose that $\widetilde{\tau}_\Omega$, defined as in (2.7), is strictly positive for all $\Omega \in \mathcal{S}_{adm}$. In addition, we suppose that the mappings $\Omega \mapsto [\mathbf{M}_\Omega]_{i,j}$, $\Omega \mapsto [\mathbf{b}_\Omega]_i$, and $\Omega \mapsto c_\Omega$ admit a shape derivative at Ω for all $i, j \in \{1, \ldots, N\}$ and that all eigenvalues of $\mathbf{M}_\Omega$ are distinct, strictly positive, and larger than a positive constant β independent from Ω.*

Then, $\Phi(\Omega)$ can be written as the cumulative distribution function as $\Phi(\Omega) = F_{T_\Omega}\left(\frac{\widetilde{\tau}_\Omega}{\beta}\right)$, where T_Ω is a random variable such that

$$T_\Omega \sim \widetilde{\chi^2}\left(\mathbf{1}; \boldsymbol{\mu}_\Omega \odot \boldsymbol{\mu}_\Omega; \boldsymbol{\lambda}_\Omega\right)$$

with $\boldsymbol{\lambda}_\Omega$ being the vector of the eigenvalues of $\mathbf{M}_\Omega$ and $\boldsymbol{\mu}_\Omega = \left(\mathbf{h} + \mathbf{M}_\Omega^{-1}\mathbf{b}_\Omega\right)$. Moreover, $\Phi()$ is shape-differentiable at Ω, and its derivative can be expressed as

$$(3.26)\quad \frac{\mathrm{d}}{\mathrm{d}\Omega}\left[\Phi\left(\Omega\right)\right](\boldsymbol{\theta}) = \left(\sum_{k=0}^{\infty} \mathbf{p}^k F_{\chi^2(2k+N)}\left(\frac{\widetilde{\tau}_\Omega}{\beta}\right)\right) \cdot \frac{\mathrm{d}}{\mathrm{d}\Omega}\left[\boldsymbol{\lambda}_\Omega\right](\boldsymbol{\theta})$$
$$+\left(\sum_{k=0}^{\infty} \mathbf{q}^k F_{\chi^2(2k+N)}\left(\frac{\widetilde{\tau}_\Omega}{\beta}\right)\right) \cdot \frac{\mathrm{d}}{\mathrm{d}\Omega}\left[\boldsymbol{\mu}_\Omega\right](\boldsymbol{\theta}) + \frac{1}{\beta}\left(\sum_{k=0}^{\infty} \gamma_k f_{\chi^2(2k+N)}\left(\frac{\widetilde{\tau}_\Omega}{\beta}\right)\right)\frac{\mathrm{d}}{\mathrm{d}\Omega}\left[\widetilde{\tau}_\Omega\right](\boldsymbol{\theta}).$$

Once again, the components of $\mathbf{p}^k$ *and* $\mathbf{q}^k$ *are the coefficients appearing in the decomposition of* $F_{T_\Omega}\left(\widetilde{\tau}_\Omega\right)$ *expressed as in Lemma 3.4, while* $\frac{\mathrm{d}}{\mathrm{d}\Omega}\left[\widetilde{\tau}_\Omega\right](\boldsymbol{\theta})$ *is as in (2.14), and the shape derivatives of* $\boldsymbol{\lambda}_\Omega$*,* $\boldsymbol{\mu}_\Omega$*, and* $\widetilde{\tau}$ *are*

$$\frac{\mathrm{d}}{\mathrm{d}\Omega}\left[\boldsymbol{\lambda}_\Omega\right](\boldsymbol{\theta}) = \operatorname{diag}\left\{\mathbf{Q}_\Omega{}^{\mathrm{T}}\frac{\mathrm{d}}{\mathrm{d}\Omega}\left[\mathbf{M}_\Omega\right](\boldsymbol{\theta})\,\mathbf{Q}_\Omega\right\};$$
$$\frac{\mathrm{d}}{\mathrm{d}\Omega}\left[\mu_{\Omega i}\right](\boldsymbol{\theta}) = \sum_{j\neq i}\left(\frac{1}{\lambda_{\Omega,i}-\lambda_{\Omega,i}}\left(\mathbf{v}^{i\,\mathrm{T}}\frac{\mathrm{d}}{\mathrm{d}\Omega}\left[\mathbf{M}_\Omega\right](\boldsymbol{\theta})\,\mathbf{v}^j\right)\left(\mathbf{v}^{j\,\mathrm{T}}\left(\mathbf{h}+\mathbf{M}_\Omega{}^{-1}\mathbf{b}_\Omega\right)\right)\right)$$
$$+\,\mathbf{v}^{i\,\mathrm{T}}\left(\mathbf{M}_\Omega{}^{-1}\frac{\mathrm{d}}{\mathrm{d}\Omega}\left[\mathbf{b}_\Omega\right](\boldsymbol{\theta}) + \mathbf{M}_\Omega{}^{-1}\frac{\mathrm{d}}{\mathrm{d}\Omega}\left[\mathbf{M}_\Omega\right](\boldsymbol{\theta})\,\mathbf{M}_\Omega{}^{-1}\mathbf{b}_\Omega\right)\qquad \textit{for all } i \in \{1,\ldots,N\}.$$

Proof. The proof of the identity $\Phi\left(\Omega\right) = F_{T_\Omega}\left(\frac{\widetilde{\tau}_\Omega}{\beta}\right)$ is analogous to the proof of (3.12) in Proposition 3.5. In order to compute the shape derivative of $\Phi\left(\cdot\right)$ at Ω, we recall that the identity (2.17) holds for any differentiable shape functional $\mathcal{S}_{adm} \to \mathbb{R}$ any Lipschitz-continuous domain, and any mapping $\boldsymbol{\xi} : [0,\delta] \to \mathrm{W}^{1,\infty}\left(\mathbb{R}^d;\mathbb{R}^d\right)$. Thus, taking as deformation field $\boldsymbol{\xi}(t) = t\boldsymbol{\theta}$, we have

$$\frac{\mathrm{d}}{\mathrm{d}\Omega}\left[\Phi\left(\Omega\right)\right](\boldsymbol{\theta}) = \frac{\mathrm{d}}{\mathrm{d}t}\Phi\left(\Omega\circ\left(\mathbb{I}+t\boldsymbol{\theta}\right)\right)\Big|_{t=0} = \frac{\mathrm{d}}{\mathrm{d}t}F_{T_{\Omega\circ(\mathbb{I}+t\boldsymbol{\theta})}}\left(\widetilde{\tau}_\Omega\right)\Big|_{t=0}.$$

We denote $T(t) = T_{\Omega\circ(\mathbb{I}+t\boldsymbol{\theta})}$, $\boldsymbol{\lambda}(t) = \boldsymbol{\lambda}_{\Omega\circ(\mathbb{I}+t\boldsymbol{\theta})}$, $\boldsymbol{\mu}(t) = \boldsymbol{\mu}_{\Omega\circ(\mathbb{I}+t\boldsymbol{\theta})}$, and $\widetilde{\tau}(t) = \widetilde{\tau}_{\Omega\circ(\mathbb{I}+t\boldsymbol{\theta})}$. Equation (3.26) and the expressions of the shape derivatives of $\boldsymbol{\lambda}_\Omega$, $\boldsymbol{\mu}_\Omega$ and $\widetilde{\tau}_\Omega$ are found using Proposition 3.5 and the identity (2.17). ∎

4. Numerical simulations.

4.1. Presentation of the algorithm. The theoretical results stated in the previous section have been applied to the shape optimization of a cantilever and a bridge-like structure. In both examples, we considered the structure to be composed by an isotropic linear elastic material, subject to random mechanical loads. For the two structures, we aimed to minimize their mass under constraints on the probability of the compliance to exceed a threshold. We recall that the compliance of an elastic structure Ω is defined as the work of the external mechanical load $\mathbf{g}$ and can be expressed as a quadratic function of the displacement $\mathbf{u}_{\Omega,\mathbf{g}}$ as

$$(4.1)\qquad \mathcal{C}\left(\Omega,\mathbf{u}_{\Omega,\mathbf{g}}\right) = \int_{\Gamma_\mathrm{N}} \mathbf{g}\cdot\mathbf{u}_{\Omega,\mathbf{g}}\,\mathrm{ds} = \int_\Omega \boldsymbol{\sigma}\left(\mathbf{u}_{\Omega,\mathbf{g}}\right) : \nabla\mathbf{u}_{\Omega,\mathbf{g}}\,\mathrm{d}\mathbf{x}.$$

The problems considered in the following can be resumed by the following structure:

$$
(4.2)\quad \left|\begin{array}{l}
\text{Find the admissible shape } \Omega \in \mathcal{S}_{adm} \text{ minimizing } \mathtt{J} = \mathrm{Vol}\,(\Omega) \text{ under the constraint} \\
\qquad \mathtt{H}(\Omega) = \dfrac{\mathbb{P}\left[\mathcal{C}\left(\Omega, \mathbf{u}_{\Omega,\mathbf{g}}(\omega)\right) > \tau\right]}{\bar{p}} - 1 \le 0, \\
\text{where the state } \mathbf{u}_{\Omega,\mathbf{g}} \text{ satisfies the state equation (2.2) for almost all } \omega \in \mathcal{O} \\
\text{with } \mathbf{g} \in \mathrm{L}^2\left(\mathcal{O}, \mathbb{P}; \mathrm{L}^2\left(\Gamma_{\mathrm{N}}\right)\right) \text{ satisfying (2.1) and } \mathbf{X} = (X_1, \ldots, X_N)^{\mathrm{T}} \sim \mathcal{N}\left(\boldsymbol{\mu}, \mathbb{I}\right).\text{‘}
\end{array}\right.
$$

All simulations have been performed under the python-based *sotuto* platform proposed by Dapogny and Feppon in [15], which relies on the *nullspace optimization* algorithm [23, 24]. The computation of the elastic displacements and the adjoint stateshas been performed using the finite-element solver *FreeFem++* [26]. We represented the domains by the means of conforming meshes obtained using the implicit-domain remeshing tool of *mmg* [13, 14], coupled to the level-set representation of the shapes [3, 44]. The advection of the level-set function is handled by the *advect* library [6], while the computation of the signed distance function is performed by *mshdist* [16] – both libraries are part of the *ISCD toolbox* [43]. The simulations have been ran on a Virtualbox virtual machine Linux with 1GB of dedicated memory, installed on a Dell PC equipped with a 2.80 GHz Intel i7 processor.

4.2. Optimization of a 3d cantilever. We consider Ω to be the cantilever structure represented as seen in Figure 1, subject to an uncertain mechanical load $\mathbf{g}$ perpendicular to the main axis of the cantilever. The load is applied on the region of the boundary denoted by Γ_{N}, while the structure is clamped on the four corner regions marked as Γ_{D}. We suppose that the cantilever has a square cross section with side length ℓ_s, and its length along the x axis is ℓ_x. Moreover, we consider the structure to made up of an elastic material characterized by a Young's modulus E and a Poisson's ratio ν. We consider the uncertain load to have the structure

$$
\mathbf{g}(\omega) = \overline{g}_x X_x(\omega)\mathbf{e}_x + \overline{g}_y X_y(\omega)\mathbf{e}_y + \big(\overline{g}_0 + \overline{g}_z X_z(\omega)\big)\mathbf{e}_z, \tag{4.3}
$$

where X_x, X_y and X_z are real valued Gaussian random variables, $\{\mathbf{e}_x, \mathbf{e}_y, \mathbf{e}_z\}$ is the canonical basis of $\mathbb{R}^3$, and $\overline{g}_x$, $\overline{g}_y$, $\overline{g}_z$ and $\overline{g}_0$ are deterministic forces. The geometric and material properties of the structure are collected in Table 1.

We performed three different simulations. In the first two, we solved the optimization problem (4.2) for different distributions of the random vector $\mathbf{X} = [X_x,\ X_y,\ X_z]^{\mathrm{T}}$. In **case A**, we consider a random load $\mathbf{g}_A$ orthogonal to the main axis of the cantilever, which is symmetric in the y direction, but on average a traction in the $-z$ direction with modulus $\overline{g}_0$. In **case B**, the stochastic term in the direction y in the load $\mathbf{g}_B$ is replaced by a random traction-compression force parallel to the main axis x. The third simulation considered is fully deterministic: $\mathbf{g}_D = \overline{g}_0\mathbf{e}_z$ is the only load applied to Γ_{N}, and the constraint $\mathtt{H}(\Omega) \le 0$ of the optimization problem (4.2) is replaced by

$$
\widetilde{\mathtt{H}}(\Omega) = \mathcal{C}\left(\Omega, \mathbf{u}_{\Omega,\mathbf{g}}(\omega)\right) - \tau \le 0.
$$

The results for the three simulations are reported in Table 2. The optimal shapes resulting from the solution of **case A**, **case B**, and the **deterministic case** are shown in Figure 2,

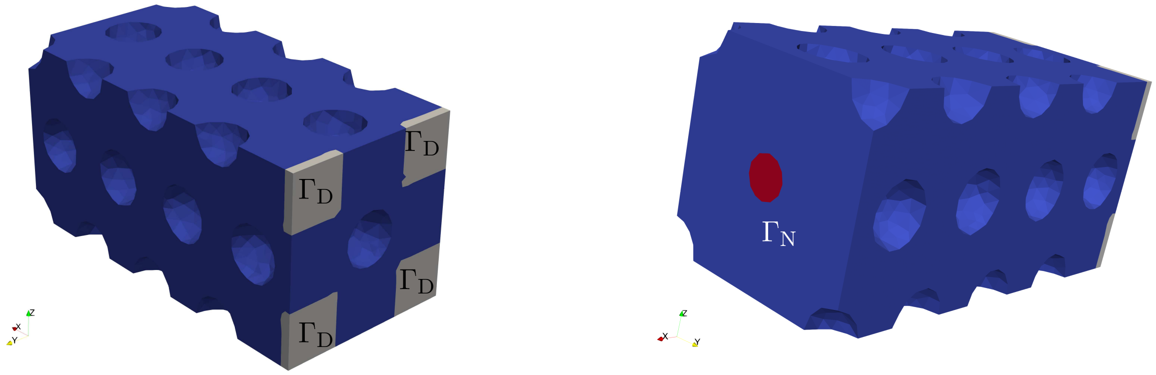

Figure 1. *Structure of the cantilever. The region Γ_{N} where the random load is applied is marked in red, while the clamping region Γ_{D} is highlighted in grey.*

Cross section length	ℓ_s	1.0 cm
Longitudinal length	ℓ_x	2.0 cm
Sidelength of Γ_{D}		0.3 cm
Radius of Γ_{N}		0.1 cm
Young's modulus	E	200 MPa
Poisson's ratio	ν	0.3
Horizontal load	$\overline{g}_y$	10 kPa
Vertical load	$\overline{g}_z$	10 kPa
Minimal mesh size	$h_{\mathtt{min}}$	0.025 cm
Maximal mesh size	$h_{\mathtt{max}}$	0.10 cm
Average mesh size	$h_{\mathtt{avg}}$	0.05 cm
Threshold on the compliance	τ	3×10^{-3} MPa cm^3
Bound on the probability of failure	$\bar{p}$	1.0 %

Table 1

Numerical data concerning the geometry and the mechanics of the cantilever structure of Figure 1.

Figure 3, and Figure 4, respectively. The decrease of the objective function in the three problems is shown in Figure 5a, and the trend of the constraint for **case A** and **case B** is reported in Figure 5b.

By comparing Figure 2 and Figure 3, we observe that the optimal solutions for **case A** and **case B** are quite similar, being convex hulls that are slightly reinforced on the z direction. In contrast, the solution of the deterministic problem presented in Figure 4 is radically different, showing a thin branched structure. Such difference can be explained by the fact that, on average, the cantilever is subject to a stronger mechanical load in **case A** and **case B**, therefore the corresponding optimal structures ought to be more robust in order to satisfy the constraint on the probability for the compliance to exceed the threshold τ.

Another notable difference between the deterministic and the uncertain cases concerns the speed of convergence. Indeed, Figure 5a shows that the volume of the cantilever in the

	case A	case B	Deterministic case
Number of iterations	500	500	348
Execution time	152 min 32 s	177 min 49 s	114 min 15 s
Final volume $\mathrm{Vol}\,(\Omega_{\mathrm{opt}})$	$0.4605\,\mathrm{cm}^3$	$0.4103\,\mathrm{cm}^3$	$0.0573\,\mathrm{cm}^3$
$\mathbb{P}\left[\mathcal{Q}\left(\Omega, \mathbf{u}_{\Omega,\mathbf{g}}(\omega)\right) > \tau\right]$			
Excess probability under load $\mathbf{g}_A$	0.996 %	4.005 %	59.579 %
Excess probability under load $\mathbf{g}_B$	4.726 %	0.991 %	88.293 %

Table 2

Numerical results for the optimization of the volume of a cantilever subject to uncertain mechanical loads under constraint on the probability of the compliance to exceed a threshold τ.

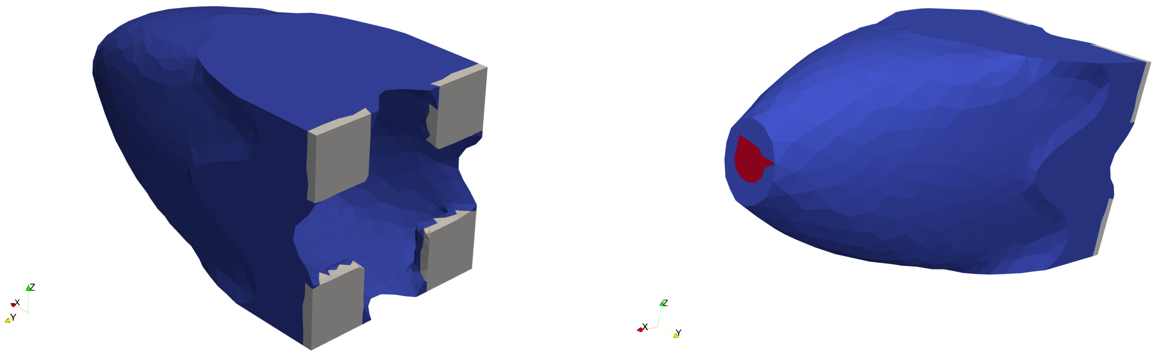

Figure 2. *Optimal shape for* ***case A****, where the applied load is* $\mathbf{g}_A(\omega) = \overline{g}_y X_y(\omega)\mathbf{e}_y + \left(\overline{g}_0 + \overline{g}_z X_z(\omega)\right)\mathbf{e}_z$.

deterministic problem converges much faster than the simulations of **case A** and **case B**. Moreover, in the deterministic case, the optimization algorithm reaches a satisfying result and stops after 349 iterations, while the rate of convergence is much slower for **case A** and **case B**. Difficulties in the convergence of the cantilever structure discussed here have also been observed in [23, Section 6.2.1].

Finally, we remark that the shapes resulting from the solution of for **case A** and **case B** comply with the constraint on the probability of failure, as shown in Table 2. The observance of the constraint, the decrease of the objective functional, and the radically different result with respect to the deterministic case justify the use of the *nullspace optimization* algorithm for the solution of Problem 4.2, and the suitability of the approach of Section 3 for the expression of $\Phi(\Omega)$ and its shape derivative.

4.3. Optimization of a 3d bridge. As a second example, we consider the optimization of the bridge structure found in Figure 6. The structure is pinned on the lower surface on its four corners, marked in light green in the picture. The pinned region, where Dirichlet boundary conditions on the displacement are applied, is denoted Γ_{D}. The upper face of the bridge is divided into five sections $\Gamma_{\mathrm{N}}^1, \ldots, \Gamma_{\mathrm{N}}^5$ of equal size. On each section Γ_{N}^i, a random load $\mathbf{g}_i \in \mathrm{L}^2\left(\mathcal{O}, \mathbb{P}; \mathrm{L}^2\left(\Gamma_{\mathrm{N}}^i\right)\right)$ is applied. We suppose that the mechanical loads are oriented

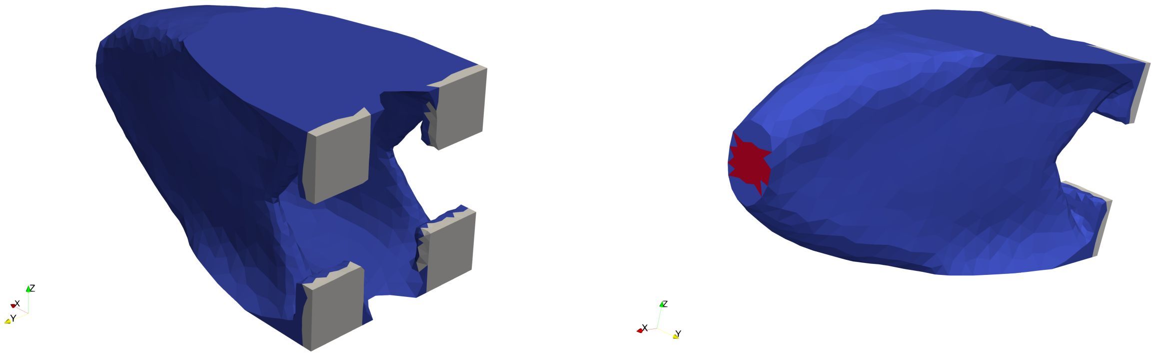

Figure 3. *Optimal shape for* ***case B****, where the applied load is* $\mathbf{g}_B(\omega) = \overline{g}_x X_x(\omega)\mathbf{e}_x + (\overline{g}_0 + \overline{g}_z X_z(\omega))\,\mathbf{e}_z$.

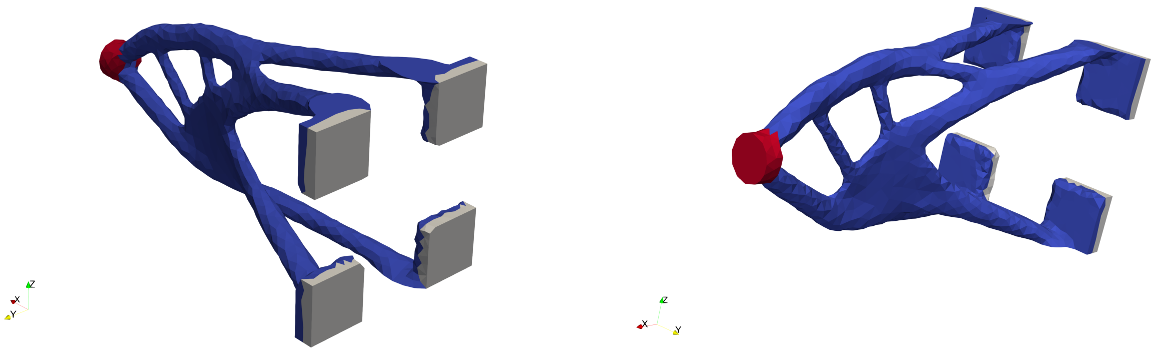

Figure 4. *Optimal shape for the* ***deterministic case****, where the mechanical load applied is* $\mathbf{g}_D = \overline{g}_0\mathbf{e}_z$.

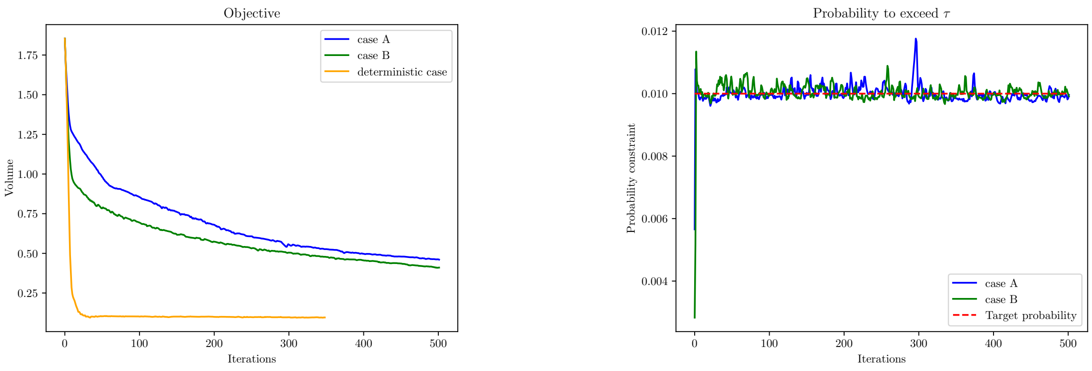

(a) Evolution of the objective function (in cm^3).

(b) Evolution of the constraint.

Figure 5. *Convergence of the objective and the constraints for the cantilever problems.*

vertically (that is along the z axis), independent from one another, and such that

$$\mathbf{g}_i(\omega) = -\overline{g}_i X_i(\omega)\mathbf{e}_z \qquad \text{on}\, {\Gamma_{\mathrm{N}}}^i \tag{4.4}$$

for all $i \in \{1, \ldots, 5\}$, where $\overline{g}_i\mathbf{e}_z$ is a deterministic vertical pressure and X_i a Gaussian random variable. The numerical parameters describing the geometry and the mechanical properties of the bridge are reported in Table 3.

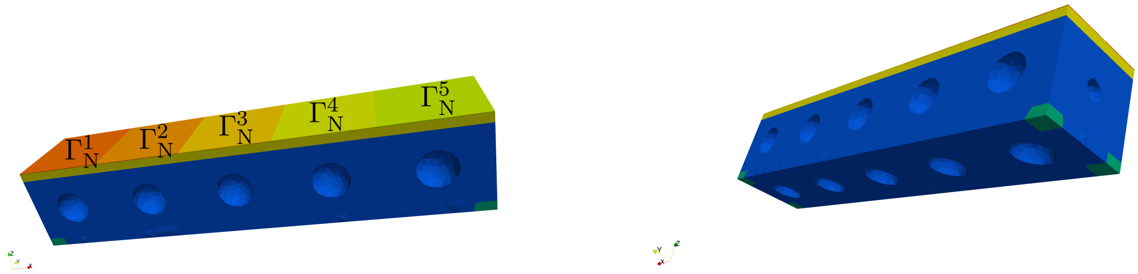

Figure 6. *Structure of the bridge. The non-optimizable supports of the bridge are marked in light green and their lower surface Γ_{D} is where Dirichlet are applied. The yellow block is non-optimizable as well, and on its upper surface five random mechanical loads are applied on the sections $\Gamma_{\mathrm{N}}^1, \ldots, \Gamma_{\mathrm{N}}^5$.*

Longitudinal length	ℓ_x	4.0 cm
Cross section length	ℓ_y	1.0 cm
Height	ℓ_z	1.0 cm
Sidelength of Γ_{D}		0.2 cm
Sidelength of each Γ_{N}^i		1.0 cm
Young's modulus	E	200 MPa
Poisson's ratio	ν	0.3
Vertical load	$\overline{g}_i$	1 MPa
Minimal mesh size	$h_{\mathtt{min}}$	0.10 cm
Maximal mesh size	$h_{\mathtt{max}}$	0.05 cm
Average mesh size	$h_{\mathtt{avg}}$	0.06 cm
Threshold on the compliance	τ	1×10^{-1} MPa cm^3
Bound on the probability of failure	$\bar{p}$	1.0 %

Table 3

Numerical data concerning the geometry and the mechanics of the cantilever structure of Figure 6.

We suppose that $\mathbf{X} = [X_1, \ldots, X_5]$ is a Gaussian random vector with covariance matrix equal to the identity where all random variables X_i to have a mean equal to -1.0. Thus, the mean of $\mathbf{X}$ corresponds to an average compression load of 1.0 MPa on each of the five sections of the bridge. We consider the shape shown in Figure 6 as initial condition, and the optimized shape is reported in Figure 7. The optimization algorithm needed only 100 iterations, which results in a computation time of 126 min and 54 s. The volume $\mathrm{Vol}(\Omega_{\mathrm{opt}})$ of the final shape is $1.217\,\mathrm{cm}^3$ and the excess probability $\mathbb{P}\left[\mathcal{Q}\left(\Omega, \mathbf{u}_{\Omega,\mathbf{g}}(\omega)\right) > \tau\right]$ equals to 0.961%. The trends of the objective and the constraint are presented in Figure 8a and Figure 8b. As for the cantilever in Subsection 4.2, these results validate that the constraint on the probability of failure is upheld. Moreover, Figure 8a show that the convergence of the objective function is faster for the bridge than the cantilever.

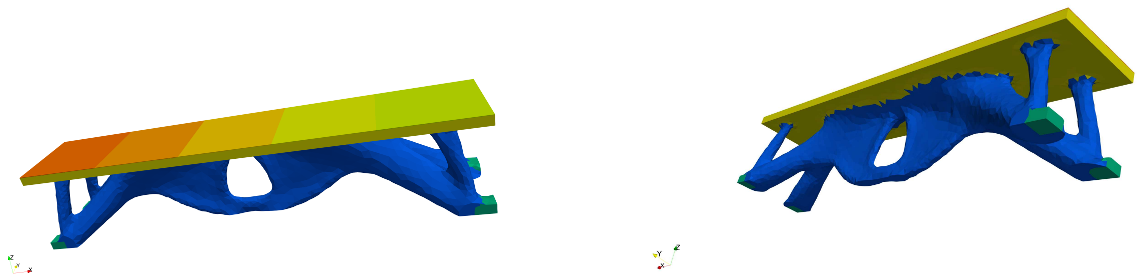

Figure 7. *Result of the shape optimization of the bridge for the non-centered case.*

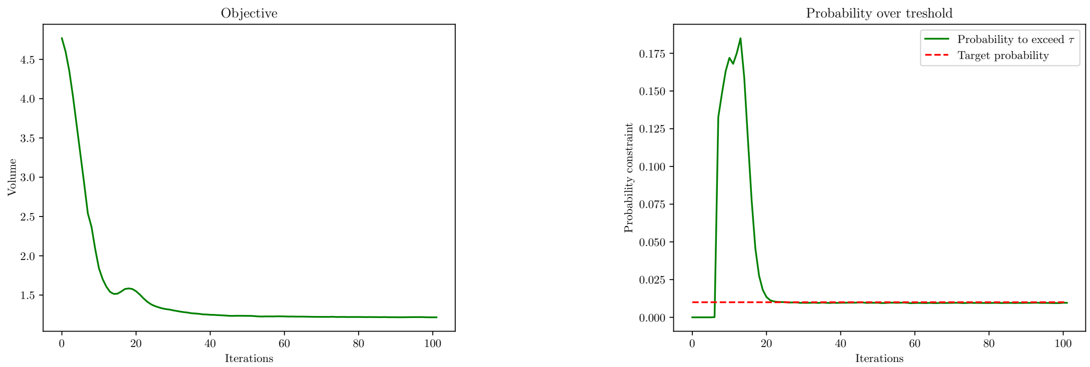

(a) Evolution of the objective function (in cm^3).

(b) Evolution of the constraint.

Figure 8. *Evolution of the objective and constraint functions through the execution of the algorithm when optimizing a bridge-like structure.*

5. Conclusion. In the present article, we presented a numerical approach to minimize the probability of failure of elastic materials under random loadings. The objective under consideration is non-smooth with respect to the random variables as it admits a kink induced from the modulus function. However, the kink can be resolved in case of a quadratic shape functional. We have proven the shape differentiability in a rather general setting and provided then an efficient gradient based algorithm in case of Gaussian random fields. Numerical results in three spatial dimensions have been presented to show the feasibility of our approach.

REFERENCES

[1] Gregoire Allaire. *Conception optimale de structures*, volume 58 of *Mathématiques & Applications*. Springer, Berlin-Heidelberg, 2007.

[2] Grégoire Allaire and Charles Dapogny. A deterministic approximation method in shape optimization under random uncertainties. *SMAI Journal of Computational Mathematics*, 1:83–143, 2015.

[3] Grégoire Allaire, Charles Dapogny, and Pascal Frey. A mesh evolution algorithm based on the level set method for geometry and topology optimization. *Structural and Multidisciplinary Optimization*, 48(4):711–715, 2013.

[4] Dean A. Bodenham and Niall M. Adams. A comparison of efficient approximations for a weighted sum of chi-squared random variables. *Statistics and Computing*, 26(4):917–928, 2016.

[5] Michael J. Buckley and Geoffrey K. Eagleson. An Approximation to the Distribution of Quadratic Forms in Normal Random Variables. *Australian Journal of Statistics*, 30A(1):150–159, 1988.

[6] Cuc Bui, Charles Dapogny, and Pascal Frey. An accurate anisotropic adaptation method for solving the level set advection equation. *International Journal for Numerical Methods in Fluids*, 70(7):899–922, 2012.

[7] Shikui Chen and Wei Chen. A new level-set based approach to shape and topology optimization under geometric uncertainty. *Structural and Multidisciplinary Optimization*, 44(1):1–18, July 2011.

[8] Tong Chen and Thomas Lumley. Numerical evaluation of methods approximating the distribution of a large quadratic form in normal variables. *Computational Statistics & Data Analysis*, 139:75–81, 2019.

[9] Sergio Conti, Martin Held, Harald Pach, Martin Rumpf, and Rüdiger Schultz. Shape optimization under uncertainty. a stochastic programming approach. *SIAM Journal on Optimization*, 19(4):1610–1632, 2009.

[10] Marc Dambrine, Charles Dapogny, and Helmut Harbrecht. Shape optimization for quadratic functionals and states with random right-hand sides. *SIAM Journal on Control and Optimization*, 53(5):3081–3103, 2015.

[11] Marc Dambrine, Helmut Harbrecht, and Bénédicte Puig. Computing quantities of interest for random domains with second order shape sensitivity analysis. *ESAIM: Mathematical Modelling and Numerical Analysis*, 49(5):1285–1302, 2015.

[12] Marc Dambrine, Helmut Harbrecht, and Bénédicte Puig. Incorporating knowledge on the measurement noise in electrical impedance tomography. *ESAIM: Control, Optimisation and Calculus of Variations*, 25:84, 2019.

[13] Charles Dapogny, Cécile Dobrzynski, and Pascal Frey. Three-dimensional adaptive domain remeshing, implicit domain meshing, and applications to free and moving boundary problems. *Journal of Computational Physics*, 262:358–378, 2014.

[14] Charles Dapogny, Cécile Dobrzynski, Pascal Frey, and Algiane Froehly. Mmg Platform – Upgrade your meshes.

[15] Charles Dapogny and Florian Feppon. Shape optimization using a level set based mesh evolution method: an overview and tutorial, December 2022.

[16] Charles Dapogny and Pascal Frey. Computation of the signed distance function to a discrete contour on adapted triangulation. *Calcolo*, 49(3):193–219, 2012.

[17] Robert B. Davies. Numerical inversion of a characteristic function. *Biometrika*, 60(2):415–417, 1973.

[18] Robert B. Davies. Algorithm AS 155: The distribution of a linear combination of χ^2 random variables. *Journal of the Royal Statistical Society. Series C (Applied Statistics)*, 29(3):323–333, 1980.

[19] Michel C. Delfour and Jean-Paul Zolesio. *Shapes and Geometries: Metrics, Analysis, Differential Calculus, and Optimization*. Advances in Design and Control. SIAM, Philadelphia, 2nd edition, 2011.

[20] Pierre Duchesne and Pierre Lafaye De Micheaux. Computing the distribution of quadratic forms: Further comparisons between the Liu–Tang–Zhang approximation and exact methods. *Computational Statistics & Data Analysis*, 54(4):858–862, 2010.

[21] Peter D. Dunning and H. Alicia Kim. Robust topology optimization: Minimization of expected and variance of compliance. *AIAA Journal*, 51(11):2656–2664, 2013.

[22] Richard W. Farebrother. Algorithm AS 204: The distribution of a positive linear combination of χ^2 random variables. *Journal of the Royal Statistical Society. Series C (Applied Statistics)*, 33(3):332–339, 1984.

[23] Florian Feppon. *Optimisation topologique de systèmes multiphysiques.* PhD thesis, Université Paris Saclay (COmUE), December 2019.

[24] Florian Feppon, Grégoire Allaire, and Charles Dapogny. Null space gradient flows for constrained optimization with applications to shape optimization. *ESAIM: Control, Optimisation and Calculus of Variations*, 26:90, 2020.

[25] Peter Hall. Chi squared approximations to the distribution of a sum of independent random variables. *The Annals of Probability*, 11(4):1028–1036, 1983.

[26] Frédéric Hecht. New development in freefem++. *Journal of Numerical Mathematics*, 20(3-4):1–14, 2012.

[27] Antoine Henrot and Michel Pierre. *Shape Variation and Optimization: A Geometrical Analysis.* Number 28 in Tracts in Mathematics. European Mathematical Society, Zurich, 2018.

[28] Jean-Pierre Imhof. Computing the distribution of quadratic forms in normal variables. *Biometrika*, 48(3-4):419–426, 1961.

[29] Diego Kuonen. Saddlepoint approximations for distributions of quadratic forms in normal variables. *Biometrika*, 86(4):929–935, 1999.

[30] Boyan S. Lazarov, Mattias Schevenels, and Ole Sigmund. Topology optimization with geometric uncertainties by perturbation techniques. *International Journal for Numerical Methods in Engineering*, 90:1321–1336, 2012.

[31] Bruce G. Lindsay, Ramani S. Pilla, and Prasanta Basak. Moment-based approximations of distributions using mixtures: Theory and applications. *Annals of the Institute of Statistical Mathematics*, 52(2):215–230, 2000.

[32] Huan Liu, Yongqiang Tang, and Hao Helen Zhang. A new chi-square approximation to the distribution of non-negative definite quadratic forms in non-central normal variables. *Computational Statistics & Data Analysis*, 53(4):853–856, 2009.

[33] Thomas Lumley, Jennifer Brody, Gina Peloso, Alanna Morrison, and Kenneth Rice. FastSKAT: Sequence kernel association tests for very large sets of markers. *Genetic Epidemiology*, 42(6):516–527, 2018.

[34] Jan R. Magnus. On differentiating eigenvalues and eigenvectors. *Econometric Theory*, 1(2):179–191, 1985.

[35] Olivier Pironneau. *Optimal Shape Design for Elliptic Systems.* Springer, New York, 1983.

[36] Herbert Robbins and Edwin J. G. Pitman. Application of the method of mixtures to quadratic forms in normal variates. *The Annals of Mathematical Statistics*, 20(4):552–560, 1949.

[37] Harold Ruben. Probability content of regions under spherical normal distributions, IV: The distribution of homogeneous and non-homogeneous quadratic functions of normal variables. *The Annals of Mathematical Statistics*, 33(2):542–570, 1962.

[38] Walter Rudin. *Principles of Mathematical Analysis.* International Series in Pure and Applied Mathematics. McGraw-Hill, New York, third edition edition, 1976.

[39] Franklin E. Satterthwaite. An approximate distribution of estimates of variance components. *Biometrics Bulletin*, 2(6):110–114, 1946.

[40] Claudia Schillings, Stephan Schmidt, and Volker Schulz. Efficient shape optimization for certain and uncertain aerodynamic design. *Computers & Fluids*, 46(1):78–87, 2011.

[41] John Sheil and Iognaid O'Muircheartaigh. Algorithm AS 106: The distribution of non-negative quadratic forms in normal variables. *Journal of the Royal Statistical Society. Series C (Applied Statistics)*, 26(1):92–98, 1977.

[42] Jacques Simon and François Murat. Sur le contrôle par un domaine géométrique. *Laboratoire d'Analyse Numérique de l'Université de Paris VI*, January 1976.

[43] ISCD Sorbonne. ISCD toolbox.

[44] Nico P. van Dijk, Kurt Maute, Matthijs Langelaar, and Fred van Keulen. Level-set methods for structural topology optimization: a review. *Structural and Multidisciplinary Optimization*, 48(3):437–472, 2013.